SOME NEW APPLICATIONS OF SUPERCAPACITORS IN POWER ELECTRONIC SYSTEMS

A Thesis

by

LEONARDO MANUEL PALMA FANJUL

Submitted to the Office of Graduate Studies of
Texas A&M University
in partial fulfillment of the requirements for the degree of

MASTER OF SCIENCE

August 2003

Major Subject: Electrical Engineering

SOME NEW APPLICATIONS OF SUPERCAPACITORS IN POWER ELECTRONIC SYSTEMS

A Thesis

by

LEONARDO MANUEL PALMA FANJUL

Submitted to Texas A&M University
in partial fulfillment of the requirements
for the degree of

MASTER OF SCIENCE

Approved as to style and content by:

Prasad Enjeti (Chair of Committee)	Hamid Toliyat (Member)
Jo Howze (Member)	Emil Straube (Member)
Chanan Singh (Head of Department)	

August 2003

Major Subject: Electrical Engineering

ABSTRACT

Some New Applications of Supercapacitors in Power Electronic Systems**.**

(August 2003)

Leonardo Manuel Palma Fanjul, B.S., Universidad de Concepción, Concepción, Chile

Chair of Advisory Committee: Dr. Prasad Enjeti

This thesis explores some new applications in power electronics for supercapacitors. This involves the design and development of dc-dc converters to interface the supercapacitor banks with the rest of the power electronic system. Two applications for supercapacitors are proposed and analyzed. The first application is aimed at high power applications such as motor drives. The proposed approach compensates the effect of voltage sags in the dc link of typical adjustable speed drives, thus reducing speed fluctuations in the motor and eliminating the possibility of nuisance tripping on the drive control board. The second approach presented in this thesis explores the use of supercapacitors to extend run-time for mobile devices such as laptop computers and hand held devices. Three possible approaches are explored: a) Supercapacitors connected directly across the battery; b) Battery-inductor-supercapacitor connection; and c) Supercapacitor, and battery connected via a DC-DC converter. Analytical models, simulation and experimental results on a typical laptop computer are presented.

TABLE OF CONTENTS

Page

CHAPTER Page

LIST OF FIGURES

FIGURE Page

FIGURE Page

FIGURE Page

LIST OF TABLES

CHAPTER I

INTRODUCTION

1.1. Introduction

Modern power electronics began with the advent of the first power semiconductor devices in the 1950's. Since then many inventions of devices, converter circuits, controls, and applications have enriched the field. Since the early 1980's power electronics has emerged as an important discipline in electrical engineering due to the introduction of new switching devices and increasing popularity. Its use is growing extensively and power electronics systems can be found in practically any industrial, commercial, residential, aerospace, and military application. Moreover, recently power electronics has gain a special significance due to energy conservation concerns and the more efficient energy use made by power electronics. The core of a power electronics apparatus consists of a converter built on an array of power semiconductor switching devices that work under the guidance of control electronics.

Power electronics systems or power processors almost in every topology, with the exception of very special cases such as matrix converters, have the need of energy storage devices to provide energy backup and decoupling between different power conversion stages.

This thesis follows the style of *IEEE Transactions on Industry Applications.*

Traditionally due to their low cost the most commonly used storage devices are electrolytic capacitors and batteries, but they have some drawbacks such as size, performance and life. There are several new energy storage technologies available today such as flywheels and supercapacitors that appear to be very promising options to the traditional energy storage devices. Among these new energy storage devices supercapacitors appear to be a good option for applications that require high power densities and fast transient response, and all this in a reduced volume.

Supercapacitors are polarized devices, as are conventional electrolytic capacitors, but they differ in that supercapacitors have capacitance values ranging from 1 Farad to 2700 Farads and their equivalent series resistance is typically 10 times lower than conventional capacitors. There are two major drawbacks in the use of supercapacitors; the first one is their low terminal voltage. Current supercapacitor technology allows for a maximum voltage of 2.7 Volts; therefore to achieve the voltage levels normally used in power conversion several supercapacitor cells have to be stacked in series or an additional step-up power converter has to be included to the system. The second major drawback of supercapacitors is cost; since this is a relatively new technology the cost of supercapacitors is still high when compared to other energy storage technologies such as lead acid batteries. Currently the estimated cost per 1 Farad is around one dollar, but it is expected that in the near future this is going to fall drastically to around one cent per Farad. This will make supercapacitors a serious contender against traditional energy storage technologies.

An application of supercapacitors in power electronics systems is as backup energy storage for systems subjected to a reduction to their input voltage. This transient disturbance is commonly known and referred to as voltage sags. Power quality surveys on industrial level rank these voltage anomalies as the most common electrical disturbance on distribution systems [1]. Furthermore these disturbances are to blame for 92% of all disturbances in electric distribution systems. Especially the effect that this phenomenon has on adjustable speed drives is analyzed.

The number of battery powered applications has been multiplying as their size is becoming smaller, and therefore more portable. This size reduction has been accompanied by an increase of the number in features provided by the devices, with the consequence of higher energy requirements having a big impact on the autonomy of the devices powered by batteries. This battery autonomy is commonly referred to as run-time and is the time that the device can run from the battery until it is completely depleted. It is known that the way that batteries are discharged drastically impacts their run-time, i.e. a load with pulsating characteristics is more likely to produce a shorter run-time than a constant load. For this type of application supercapacitors can provide the transient power required by the load, and therefore soften the load requirements, whit a consequence of improved run-time.

1.2. Energy storage requirement in power converters

Power converters or power processors require energy storage devices to provide continuity of operation when the main energy source, which normally is the utility, fails

to provide the energy required to the load, and also provide decoupling between the input and output converters. The usual power converter topology is shown in figure 1 where the system is constituted by two converters connected by a energy storage element.

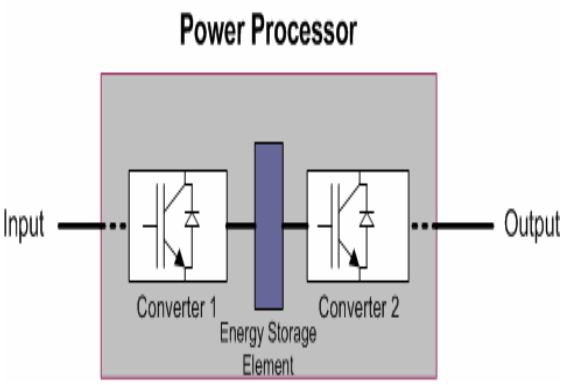

Figure 1 Typical power processor

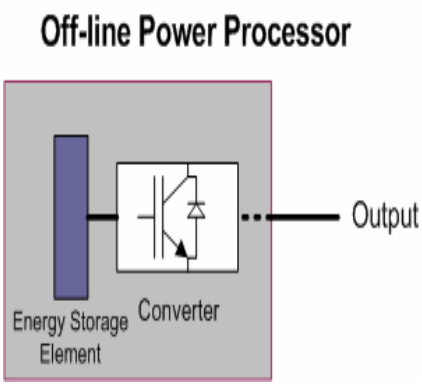

Figure 2 Typical off-line power processor

The other practical power processor topology is shown in figure 2 and it is used when the system is to work offline, and only rely on the energy stored in the energy storage element.

Traditionally these storage devices consist of batteries or bulky electrolytic capacitors which have drawbacks such as low transient response and relative high equivalent serial resistances for the case of the batteries, and low energy storage capability for the case of conventional capacitors. Recently new energy storage devices have emerged, and these new devices present several advantages to the traditional energy storage devices, such as reduced losses, and improved power densities. Also

these new devices present additional advantages because they do not contain hazardous materials harmful to the environment as do traditional batteries.

1.3. Energy storage in electrical systems

It is well known electrical energy cannot be stored in its ac form; it only can be stored in the dc form. Therefore in power electronic systems the energy storage devices are concentrated on the dc link of the converters. Although this is commonly true, over the years various indirect energy storage methods have been developed such as storing the energy as compressed air, heat, hydrogen or in rotating flywheels. Most of these storage methods are not very efficient and much of the energy is lost in the process of converting the energy from its electrical form to a different one. Among the indirect energy storage devices the flywheel appears as the most convenient and efficient.

Direct energy storage devices are those where the energy is stored without transforming the energy to a different type. These devices can be divided in two, electrical and magnetic. In the case of storing the energy electrically super capacitors are used and the energy is stored separating the electrical charge and storing it on separated electrodes. For the magnetic storage the energy is stored on the magnetic field generated by a superconducting coil. The main problem of this last storage method is that the current state of super conducting materials requires extremely low temperatures. This has the problem of working with cryogenic systems which adds complexity and size to the storage system. Also because of the extra complexity magnetic storage devices or Superconducting Magnetic Energy Storage (SEMS), as they are known have a high cost.

The different energy storage methods available are shown in figure 3, where they are grouped by direct and indirect storage, and by their specific storage reservoir.

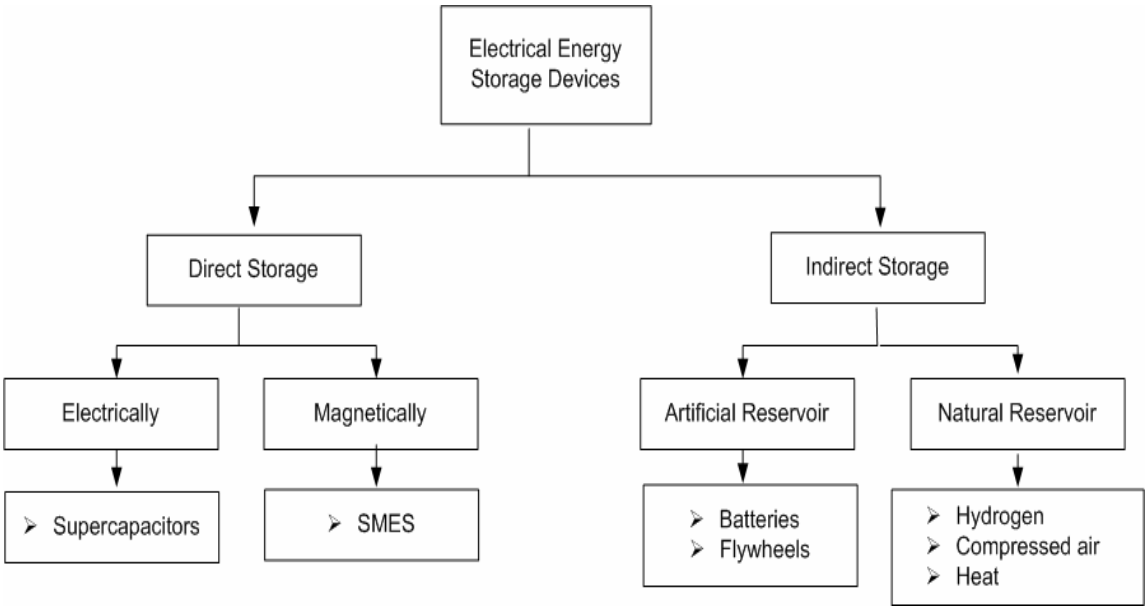

Figure 3 Electrical energy storage methods

1.4. Energy storage devices

The storage devices mentioned in the previous point are supercapacitors and flywheels. Although Flywheels have been around a long time, only recently they have evolved in to a more efficient and compact technology that can be used in power electronics systems to store energy. This is due to the development of new composite materials, which allow smaller sizes and higher rotational speeds. Such improvements result in devices capable of storing high amounts of energy on a reduced space. On the other hand the development of double layer capacitors, better known as supercapacitors or ultracapacitors, allows higher energy storage capability than traditional electrolytic

capacitors and with lower equivalent series resistance. This last feature makes this kind of capacitor a very good device for transient applications.

Because of their nature these new energy storage devices require the addition of dc-dc converters to connect them to the rest of the system. In the case of the supercapacitors the converter is required due the low terminal voltage reached by the current technology, which ranges from 2.4 to 2.7 V. When a flywheel is used as an energy storage device, the converter needed to interface to the rest of the system has to adjust the output voltage as the speed of the flywheel diminishes.

In general two factors characterize the application of an energy storage technology. One is the amount of energy that can be stored in the device. This is a characteristic of the storage device itself. Second is the rate at which energy can be transferred into or out of the storage device. This depends mainly on the peak power rating of the power conversion unit, but it is also impacted by the response rate of the storage device itself.

1.5. Trends in energy storage devices development

Energy storage devices, such as supercapacitors, flywheels, and also electro chemical batteries, are still under development. This means that in the near future their power densities and energy density capabilities are going to be improved. An estimation of the expected power/energy capabilities for these devices in the near future is shown in figure 4 [2]. From this figure is easy to see that supercapacitors will considerably increase their energy density from their actual values, which are around 5 Wh/kg to

approximately 100 Wh/kg. This makes supercapacitors a very promising energy storage technology considering that the most widely used batteries, lead acid batteries, energy density normally is about 60 Wh/kg. Integration of these energy storage technologies with power converters can provide useful applications in the area of the power quality to provide ride through power and backup energy for critical loads. Also, combining different technologies will allow for keeping the individual characteristics of each device to gain a hybrid with higher power/energy performance.

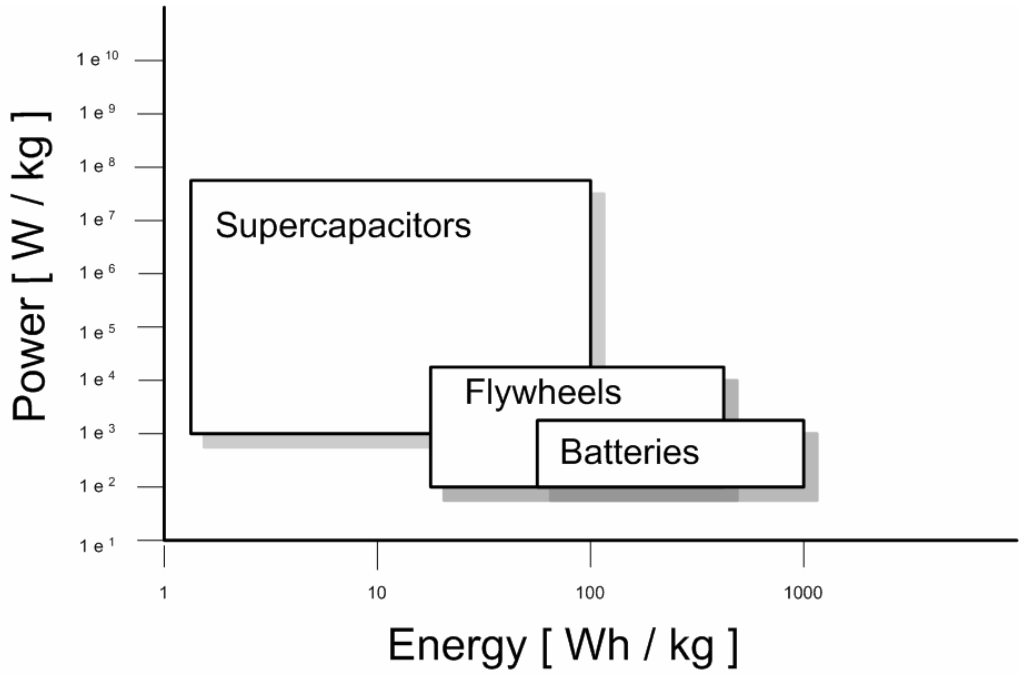

Figure 4 Power density vs. energy density for different energy storage devices

1.6. Effect of voltage sags in adjustable speed drives

Voltage sags are defined by the Institute of Electrical and Electronics Engineers, IEEE, as a decrease between 0.1 and 0.9 per unit in rms voltage at the power frequency for durations of 0.5 cycles to 1 minute. Generally voltage sags are caused by transient

events such as connecting of large loads to the system, motor starting, fast reclosing of circuit breakers, short circuits, lightning strokes on overhead lines, etc. Voltage sags normally do not cause damage to the equipment but they can disrupt the operation of sensitive electronic loads such as the control boards of adjustable speed drives, having the effect of making their protections trip. A severe sag occurrence can be defined as one where the voltage magnitude falls below the 85% of its rated value. According to power quality surveys, voltage sags are the main cause of disturbances. Also these surveys report that 68% of the disturbances are voltage sags and they are the only cause of production loss. These loses are caused by voltage sags of 13% of the rated voltage, with a duration of more than 8.3 msec. (half a cycle). In textile and paper mills brief voltage sags may potentially cause an ASD to introduce speed fluctuations which can damage the final product. Furthermore short voltage sags can produce a momentary dc-link voltage drop which can trigger the protection circuitry. That kind of nuisance tripping of an ASD used on a continuous process can cause a major disturbance in the final product.

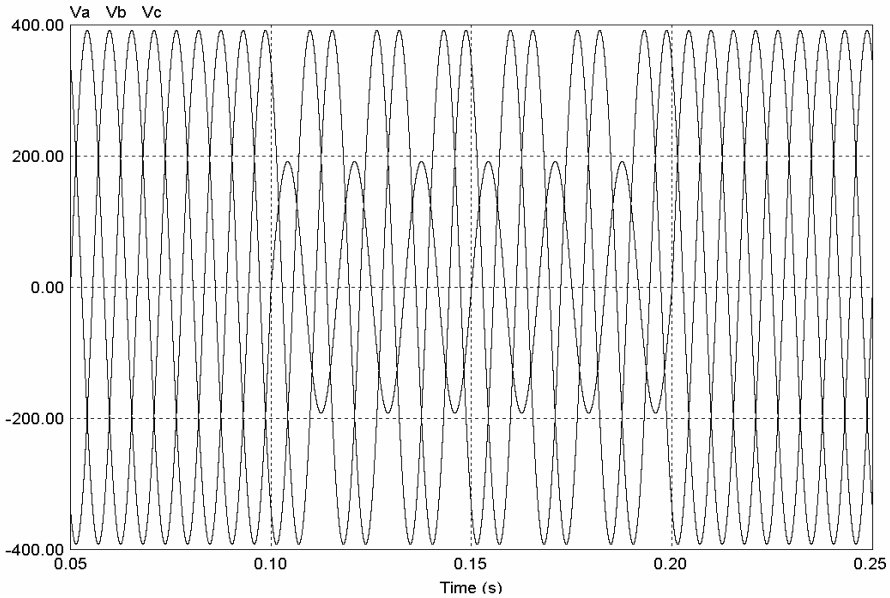

Figure 5 50% voltage sag

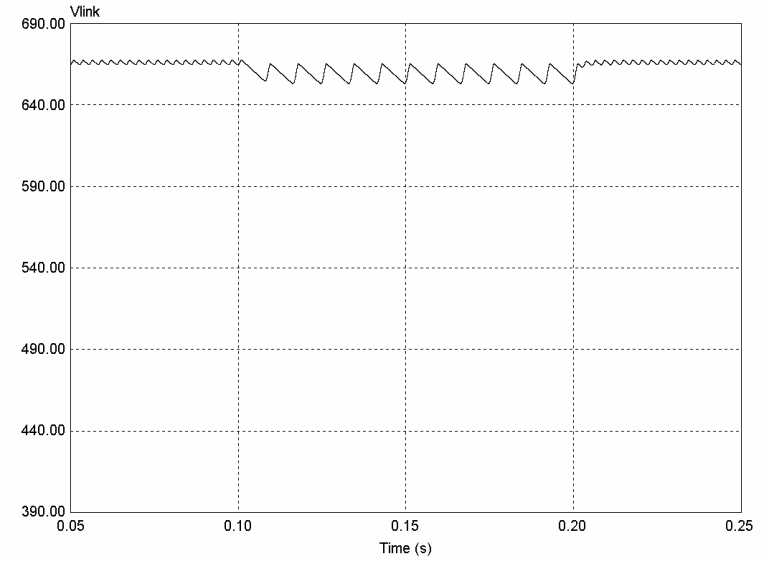

Figure 6 DC link voltage under a 50% voltage sag

.

In Figure 5 a typical single phase voltage sag can be seen. In this case the voltage drop is 50 % and it lasts for 100 μsec. The effect of this disturbance can be seen in figure

6. This reduction in the dc link voltage can cause the dc link under voltage protection to trip. To compensate the voltage sag effects in the dc link of the ASD a new compensation scheme is proposed combining a fly buck converter and a super capacitor. This scheme is capable of compensating deep voltage sags as well as short voltage interruptions.

1.7. Run-time in battery powered systems

The run-time in a battery powered portable system, such as laptops and other mobile applications, defines the span of time that the device can be under operation before the energy reserve is depleted. Mobile devices and wireless communication equipment are increasing in number and features constantly, this is driven by the anytime, anywhere computing and communications needs of today's world. All this requires batteries to deliver more performance in terms of power and energy. This can be observed from figure 7 [3], which show the steady increase in the power requirement of computer processors since 1986. Unfortunately battery manufacturers have not been able to catch-up with the increasing needs of the new devices. This is due to the dynamics and characteristics of the chemical reactions taking place in the batteries. Current battery technologies have energy densities ranging from 50 to 125 W/kg depending on the battery type as shown in figure 8. For example this means that a typical Li-Ion laptop battery normally weighting 0.4 kg can only supply the computer load, i.e. 25 Wh, for about 2 hours. Which is far from a whole office day and it does not even provide enough autonomy for running the computer during a typical airplane flight.

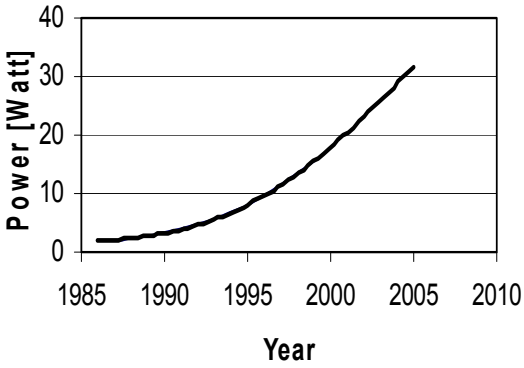

Figure 7 Microprocessor power consumption history and future trend

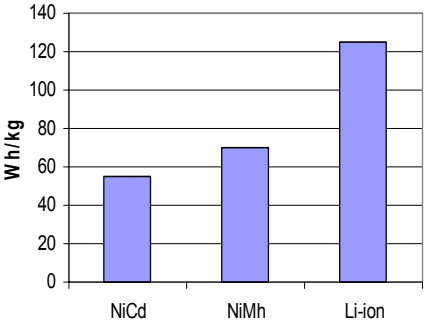

Figure 8 Battery energy densities

The traditional approach to increase the run-time of a battery powered device is done by simply increasing the number of batteries cells constituting the battery pack. This solution logically implies increasing the size and weight of the portable system, which is not acceptable since it reduces the device portability and acceptance into the market.

1.8. Previous work

The electrical model of supercapacitors has been discussed on several papers. Donald Cahela and Bruce Tatarchuk [4] presented a supercapacitor equivalent model composed by an equivalent capacitance, an equivalent series resistance and a leakage resistance. This model is accurate but the presence of a leakage resistance which is difficult to measure makes it not very practical for analysis and evaluation. A two branch electrical equivalent model for the supercapacitor has been presented by F. Belhachemi and S. Rael [5]. This model is constituted by two resistors and an equivalent capacitance and a variable capacitance. This model describes more in detail the transient response of

the capacitor but is to complex to be practical, and the model parameters are not easily measured. The simplest and most accurate model is presented by T. Smith and J. Mars [6]. This model is composed only by an equivalent capacitance and a series equivalent resistance. This simplified model is accurate and its two parameters are easy to measure.

Selecting the appropriate dc-dc topology to be used to interface the energy storage device and the load depends on the type of load and the required transient response, as said before. But in the case of supercapacitors it also requires bi-directional power flow in order to charge the devices once their stored energy has been delivered. Suitable topologies are discussed in the references by Jingquan Chen, Dragan Maksimovic [7], Alexander Rabello [8,10], Marcio Co [8,10] ,Wilson de Argano [8,9] , Ivo Barbi [8,9,10], Deepak Divan [11] and William Brumsickle [11]. The topologies presented on these references apply to specific applications and some of them do not provide bi-directional power flow. This last problem is especially important in where supercapacitors are used, because they need to be recharged after their stored energy falls bellow a certain level.

Several topologies have been proposed to provide ride through capabilities to adjustable speed drives. Jose Luis Duran and Prasad Enjeti [1] proposed a low cost approach to provide ride through for voltage sags adding three additional diodes and a boost converter to the dc-link of adjustable speed drives. The only disadvantage of this solution is that during the duration of the sag additional current is drawn from the healthy phases and that it is not able to compensate for deep sags and short interruptions.

M. Corley and J. Locker [12] proposed an approach to provide ride through using supercapacitors and a combination of a boost and buck converters connected in parallel. Although this topology is able to provide compensation for deep sags and short interruptions its main problem is that high voltage supercapacitors are needed. This because a practical boost converter is not able to generate voltages higher than twice its input voltage, and high voltage supercapacitors imply the connection of multiple capacitors cells in series increasing the cost and size of the system.

The issue of battery performance improvement is treated by T.A. Smith, J.P. Mars and G.A. Tuner [6]. Their research is focused mainly on batteries and supercapacitors used in low voltage memory backup systems, and they do not present a detailed theoretical analysis of the topic.

1.9. Research objective

The objective of this thesis is to develop some new applications in power electronics for supercapacitors. This involves the design and development of dc-dc converters to interface the supercapacitor banks with the rest of the power electronic processor. Also the characteristics of the supercapacitor impedance in frequency domain will be studied to understand its behavior when subjected to pulsating currents common in some dc-dc converter topologies.

An application of supercapacitors as backup energy storage for compensating voltage sags and short voltage interruptions for loads adjustable speed drives is presented. The proposed compensator is designed and roughly tested by means of

simulations. Later an experimental prototype is build and tested under various operating conditions to verify the effectiveness of the sag compensator.

Also the use of supercapacitors to extend battery run-time is explored. The approach used is the connection of supercapacitors and a battery in parallel, either by direct connection or by using a dc-dc converter to interface the low voltage supercapacitor cells and batteries. The frequency response of the battery-supercapacitor hybrid will be studied both analytically and experimentally. Experimental results on the battery-supercapacitor hybrid combination are obtained to verify the extension on the run-time of the system. Also experimental results on the battery-supercapacitor connection using low voltage supercapacitor cells and a dc-dc converter to interface the battery and the supercapacitor are obtained and the run-time extension will be measured.

1.10. Thesis outline

Chapter I present the need for energy storage devices in power converters and the requirements that these devices have to fulfill. Also in this chapter the possible methods that can be used to store energy in power electronic converters is discussed, and a short description of the characteristics of each device is given. Later in this chapter the expected horizons for the most promising energy storage devices are disused and analyzed. Finally the research objective of this work is presented.

In chapter II each of the most promising energy storage technologies are described and their most important characteristics discussed. A comparison between the different energy storage technologies is made.

Chapter III suitable topologies to be used to interface supercapacitors and power electronic systems are discussed and compared. Five converter topologies are presented and analyzed. From this analysis a comparison between the different converter topologies is made and conclusions are drawn.

Chapter IV discusses the application of supercapacitors as a backup energy source for adjustable speed drives when subjected to voltage sags. A simple capacitor sizing procedure for this application is developed and the required dc-dc converter to interface the supercapacitor and the adjustable speed drive is designed and tested. In the last part of this chapter conclusions are made respect to the performance of this approach to provide ride through.

Chapter V explores an approach to extend battery run-time by using a supercapacitor connected directly in parallel with the battery and by using a dc-dc converter to interface low voltage supercapacitors with batteries. The development of this converter and the testing of the two alternatives is done. In the last part of this chapter conclusions are made.

Chapter VI ends this thesis presenting the general conclusions of this work.

CHAPTER II

REVIEW OF ENERGY STORAGE DEVICES FOR POWER ELECTRONICS APPLICATIONS

2.1. Introduction

Power electronics applications require energy storage devices mainly for two reasons; the first is to use these devices as the primary energy source for power conversion, an example is portable power supplies where the energy is provided by a battery pack. The second reason is to provide an energy backup when the primary energy source, normally the utility company, fails to fulfill the load requirements, an example of this type of application are UPS systems.

These two application types for energy storage devices differ mainly from each other in the amounts of energy that the devices have to provide and in the transient dynamic response characteristics that the devices must be able to deliver. Other less important differences between these two applications involve the physical characteristics of the storage devices. This because if the energy storage device is to be used for a energy backup application the amount of space that the device can use is limited.

Energy storage devices are available in different technologies, and therefore they have also different features and characteristics that make some of them more suitable for one application than others. Differences between these technologies result in changes in

basic characteristics such as size and weight of the devices and in other more important from the electrical point of view such as dynamic response, current rating and energy and power density.

In this chapter three energy storage technologies are presented and their more important characteristics are discussed. The energy storage technologies described in this segment are the widely used and known electro-chemical batteries, the promising new technology of double layer supercapacitors and the ever improving technology of the mechanical flywheel.

2.2. Battery technology

Batteries are one of the most cost effective energy storage technologies available, where the energy is stored electrochemically. All battery systems are made up of a set of low voltage/power cells connected in series to achieve the desired terminal voltage, and in parallel to provide the desired power rating. Batteries can be charged and discharged a certain number of times given by the cycling capability of the electrodes and the chemical used as electrolyte. Currently there are various battery technologies. Where the lithium ion is becoming more popular every day, but still lead acid batteries are the most widely used due to cost issues. Key factors of batteries as energy storage devices are they high energy density, high energy capability, life span and initial cost.

As said before lead acid batteries still the most used battery technology today, mainly because of their lower initial cost. Despite these advantages this technology has

some important drawbacks such as limited cycle life, higher maintenance costs and considerably weight and size.

Other battery technologies appear promising for energy storage in power electronics applications, offering higher energy densities and improved cycle life than conventional lead acid batteries. The main problem of these other battery technologies is that the cost makes them unpractical for the typical applications in power electronics. Among these other battery technologies the most promising appear to be the nickel – cadmium, nickel – metal, and lithium – ion technologies.

Due to the chemical kinetics involved, batteries cannot handle high power levels for long time periods, and in addition rapid discharge cycles may shorten the battery life leading to early replacement. Also there are some environmental concerns related to the use of batteries due the hazardous materials contained on them, and the toxic gases generated during the charge discharge cycles. The disposal of the hazardous materials contained in the batteries implies additional costs due to strengthen environmental regulations.

2.3. Supercapacitor technology

Capacitors store electrical energy by accumulating charge on two parallel electrodes separated by a dielectric material. The capacity represents the relationship between the electric charge stored in the capacitor and the voltage between the two electrodes of the capacitor. This relationship is described by equation (1), where q represents the charge stored in the capacitor, C the capacitor value in Farads and V the

capacitor voltage. The capacitance value of a capacitor is given by the dielectric permittivity ε, the distance d separating the capacitor electrodes and the effective area of the electrodes constituting the device A; and it can be calculated using (2). The energy stored in a capacitor is a function of the capacitance value of the device and its terminal voltage; it can be calculated using (3). Where E is the energy stored in the capacitor, C is the capacitor capacitance value, and V is the capacitor terminal voltage. As can be seen from (3) the amount of energy stored in a capacitor two things can be done. One is to increase the value of the stored voltage. This value is limited by the voltage withstand strength of the dielectric material between the electrodes.

$$q = CV \tag{1}$$

$$\mathrm{C} = \frac{\varepsilon \mathrm{A}}{\mathrm{d}} \tag{2}$$

$$\mathrm{E} = \frac{1}{2}\mathrm{CV}^{2} \tag{3}$$

The other way to increase the energy stored in a capacitor is increasing its capacitance. This can be done increasing the effective area of the electrodes, increasing the permittivity of the dielectric separating the electrodes, or decreasing the distance between the two electrodes. Another important factor about capacitor technology is the equivalent series resistance or ESR. This parameter has an important effect on the turnaround efficiency when charging discharging the capacitor and on the transient response of the device.

Conventional dc capacitors have long been used as energy storage devices in power electronics converters. Common uses for these devices are applications where

pulsating bursts of energy are required and for provide limited backup energy for applications such as adjustable speed drives.

A relatively new type of capacitor is the double layer capacitor or supercapacitor. These capacitors have as main characteristics a high capacity value and extremely low ESR's when compared to traditional capacitors. The internal structure of supercapacitor differs from traditional capacitors because there is no intervening dielectric material in a supercapacitor. The reason why supercapacitors have a much higher capacitance than traditional capacitors is because of the large equivalent area of their electrodes and the small effective separation between the electrodes. One gram of the electrode material can have an equivalent area of 2000 m^2.The separation distance between an electrode and the layer of ions, the so called double layer, is in nanometer range. So applying these parameters to equation (2) it is evident how the high capacitance value is achieved.

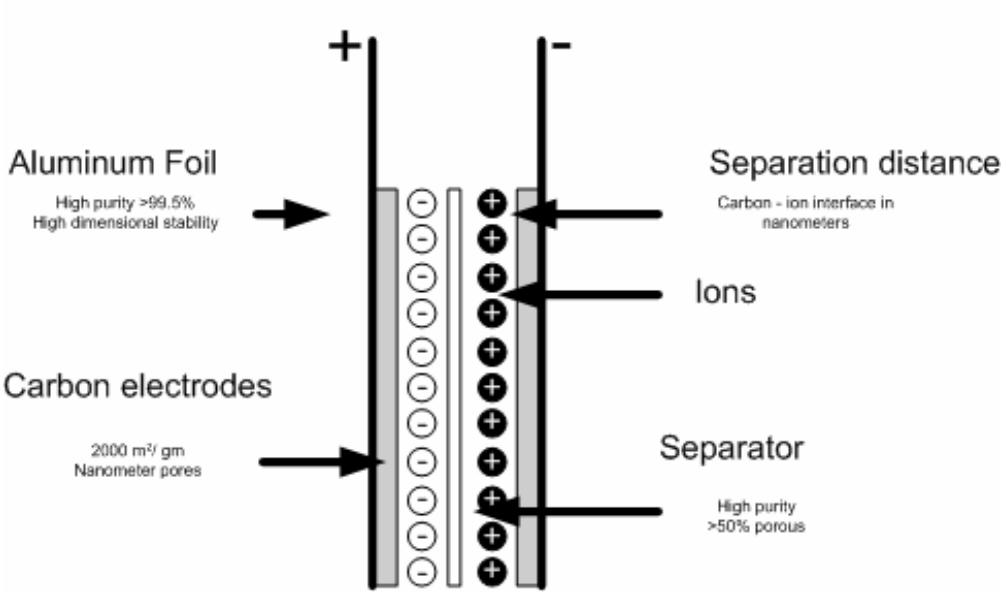

Figure 9 Double layer supercapacitor cell

In figure 9 the typical carbon double layer supercapacitor cell construction can be seen. In some way the supercapacitor construction is similar to that of a battery with two electrodes immersed in a electrolyte with a separator in between. However, unlike batteries in the case of the supercapacitor there is no chemical energy storage. There are effectively two capacitors in series within each supercapacitor cell. Each of them has a set of electrodes consisting of carbon and an adjacent electrolyte with a layer of ions.

The electrical charges are not bounded to the electrolyte, they are free to move anywhere in the electrolyte which also penetrates the pores of the carbon electrodes. The separator insulates the two electrodes whilst allowing the ions to pass through it. The electrolyte is in form of an aqueous substance which allows a maximum voltage of 1 V per cell. If an organic electrolyte is used the maximum allowable voltage is 2.5 V. The presence of impurities on the electrolyte generates chemical reactions that tend to increase the ESR and gives a finite lifetime to the supercapacitor.

2.4. Flywheel technology

Flywheels have been around for a long time, but new improvements on its technology and the need of more environmental friendly devices is giving this energy storage devices a renewed impulse. Flywheels store energy as kinetic energy on a rotating mass. This mass coupled to a motor – generator set through a shaft. In the big majority of the flywheel applications this motor-generator set is connected to a power electronic converter to provide a wide operating range. A schematic of the flywheel components is shown on figure 10.

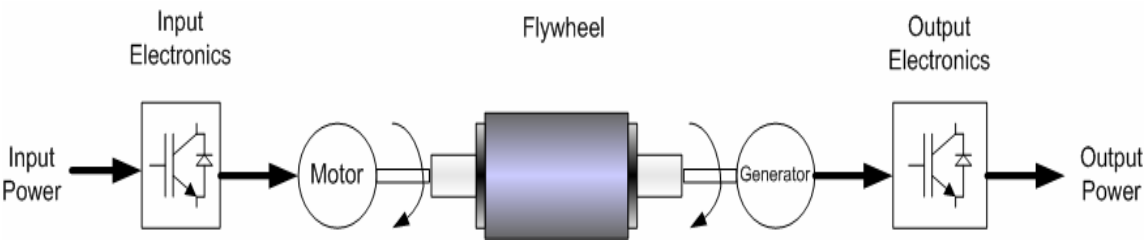

Figure 10 Flywheel system schematic

The energy stored in the device depends on the moment of inertia of the rotating mass and on the rotational velocity of the flywheel; this can be seen on equation (4). In this equation E is the kinetic energy stored in the flywheel, J is the moment of inertia of the rotating mass and ω is the rotational velocity of the flywheel.

$$E = \frac{1}{2} J \omega^2 \tag{4}$$

The moment of inertia of the rotating mass depends on the mass, radius and length of the rotational mass. Usually this mass has a cylindrical shape; in this case the moment of inertia of the mass can be calculated using equation (5).

$$J = \frac{r^2 ml}{2} \tag{5}$$

Where J is the moment of inertia of the rotating mass, r is the radius and l is the length of the cylinder.

The energy stored in the flywheel is transferred to the outside when the motor - generator operates as a generator, in this case the speed of the flywheel decreases. The

flywheel is charged when the motor – generator works as a motor increasing the rotating velocity of the flywheel.

As can be observed from equation (4) the energy storage capability of the flywheel can be improved either by increasing its moment of inertia, making spin its mass at a higher rotating velocity, or both at the same time. Two strategies than have been used to develop high power flywheels are increasing the moment of inertia by increasing the radius of the spinning mass and using materials such as iron or steel for its construction. In this case the rotational velocities used have a maximum of 10000 rpm. This kind of approach if commonly used commercially, because of the easy implementation using standard electric motors, mechanical components and power electronics. The other approach utilized is using a smaller radius and composite materials which result in a smaller moment of inertia, but allow rotational velocities as high as 100 000 rpm. This type of approach results on lighter and smaller flywheels that can store the same amount or even more energy that the previously discussed flywheel technology. Rotational loses are very important in flywheel technology, because they produce the self discharge effect. This loses are mainly produced by air drag and bearing loses, and their importance increases with the rotational velocity. Therefore high speed flywheels are mounted on evacuated containers, where the pressure is reduced to values as low as 0.1 Pa for 100 000 rpm flywheels. To reduce the bearing loses the flywheels are mounted on magnetic bearings, such as superconducting magnetic bearings. With the near eliminated rotational loses provided by the methods previously discussed flywheels

have a high charge/discharge efficiency. The peak values of the power transfer depend only on the design of the motor - generator and the power electronic converter.

The high speed operation of the flywheels require of containment units due to security concerns, because of the inherent danger of the rotational mass tearing apart due to the high centrifugal forces produced by the rotational velocity. This adds extra weight to the system which reduces their energy density [W/kg].

2.5. Comparison between energy storage technologies

As stated on the previous points in this chapter the various energy storage devices available differ in their energy densities, power densities and other important parameters such as equivalent series resistance and dynamic response time. Therefore is important to compare the different technologies in order to achieve the highest performance depending on the application on which they are going to be used.

For example, in some applications the load characteristic requires constant current, and therefore this requirement makes some technologies like batteries more suitable than the others. On the other hand when the load requirements demand a pulsating current waveform, technologies like supercapacitors are in a better position to provide energy efficiently. The differences in the energy density refer to the amount of energy stored in the device in terms of the time that it can be used. As can be observed from Table 1, currently there is a big difference between the three storage devices being discussed. Batteries appear as the best option according to energy densities 10 times higher than supercapacitors and between the same and twice times as much as flywheels. Another

important parameter when comparing energy storage devices is the power density, which measures the energy stored in the device by kg of weight. From Table 1 it is clear that supercapacitors offer higher power densities than the other two energy storage devices. In fact they provide 100 times higher power densities than batteries and about 50 times higher than flywheels.

Also important to consider in this comparison between energy storage devices is the equivalent series resistance value. A high value implies higher internal losses and bigger voltage drops at the moment when the load demands current. Consequently a lower equivalent series resistance has the benefit of lower loses and a smother voltage profile. When comparing this parameter the super capacitor appears to be the most convenient, having an ESR 10 times lower than batteries and comparable with flywheels. The different ESR values for supercapacitors, batteries and flywheels are listed on Table 2. Volume and weigh are also important parameters to consider when comparing energy storage devices, due to the size constraints present on modern power electronic converters. From this point of view also the supercapacitors offer a better alternative having a smaller volume and less weigh than the other alternatives. Flywheels also have less weigh then batteries due to the use of composite materials, but their volume is bigger because of the need of the protecting confinement vessel. Cost is always an important parameter to be considered when comparing devices. From this point of view traditional batteries such as lead acid batteries appear as having the lowest initial cost; that is without considering the maintenance costs. Their cost per Wh is less than one dollar. In the case of supercapacitors initial the cost per watt hour is around 80

dollars. Despite of having a higher initial cost, supercapacitors and flywheels have the advantage of being practically maintenance free during all their life span. This last parameter is also important to consider. The average lifespan of batteries is of five years as a maximum for batteries who are not subjected to extreme condition as low/ high temperatures and pulsating current loads. For these applications the life span of batteries is estimated to be around tree years. In the case of supercapacitors the life span is about 10 years, but this value depends on the actual charge discharge cycles that the capacitor has to withstand. Normally the number of charge discharge cycles of a supercapacitor is around 100000. Important is that this number of charge-discharge cycles do not vary because of usage under extreme environmental conditions such as very low or high temperatures or because of pulsating current loads. The life span of flywheels is also independent of the environmental conditions to which it is subjected. Also flywheel performance is independent of the type of load that is connected to its terminals. Their life span is estimated to be 20 years for advanced systems constructed using magnetic bearings and composite materials.

Table 1 Comparison between different energy storage devices

Energy Source	Energy kJ	Energy density [W/h]	Power Density [W/kg]	Price [US$]	Volume [cm3]	Weight [kg]	US$/Wh
Supercapacitors by Maxwell [13]	8,437	2.34	5000	188	593.8	0.725	80.7
Supercapacitors by Montena [14]	8,125	2.26	4300	170	486.32	0.525	75.22
Supercapacitors by Kolban [15]	20,000	5.55		500	2870.31	5	90.09
33 Ah Lead Acid Battery	1,425	360	<1000	100	3941.34	12	0.28

Table 2 Comparison between supercapacitors and battery ESR

Energy Source	ESR [mΩ]
Supercapacitor brand “A”	1.0
Supercapacitor brand “B”	0.7
Lead Acid Battery	7.0

Important to mention is that having an accurate knowledge of the state of charge of batteries is a very difficult task to accomplish. But in the case of supercapacitors or flywheels this task is much simpler. As can be seen from equation (4), to determine the amount of energy stored on a fly wheel only the rotational velocity is needed. Also from equation (3) to determine the amount of energy left on a supercapacitor only the capacitor terminal voltage has to be known.

Also important to consider is that supercapacitors and flywheels are not mature technologies, and therefore they are on continuous improvement reducing their costs and getting closer to batteries in terms of energy densities. On the other hand batteries are a proven technology widely used on power electronics applications for many years, but few improvements have been done to make their power densities higher or to reduce their size and weight. Also because of the chemical composition fewer advances can be made to reduce their ESR's or to improve their transient response.

From the previous comparison supercapacitors appear to be suitable to be used on power electronic converters as standalone energy storage devices for applications requiring pulsating burst of power or as a combination with batteries to combine the advantages of the two devices in terms of power density, energy density and equivalent ESR.

2.6. Conclusion

The three most common energy storage device technologies have been discussed in this chapter. Battery technology is a well established and widely used on numerous applications, but disadvantages like weight, size, poor power density and high equivalent series resistance make these devices not suitable for some transient applications or where volume and size are an important issue. Also due to the chemical dynamics batteries do not perform efficiently for pulsating loads.

On the other hand flywheels offer a good transient response, which depends only on the power electronic converter. Although the flywheel technology is been around for some time now, new advances on composite materials and bearing systems have reduced

their size and volume. This reduction makes flywheels a good option for energy storage in power electronic systems. Because of their energy density flywheels can compete is many applications with batteries, but they are mostly used on applications where weight is the greatest concern. This is because of cost restrictions since batteries still the most economical solution from the initial investment point of view.

Supercapacitors despite of their low energy density present a good advantage over the other two energy storage devices. This advantage is due their high power density which makes them especially suitable for loads demanding pulsating currents. Also this energy storage technology present a good advantage from the internal looses point of view because of their very low equivalent series resistance. Supercapacitors are also small in size and have less weight than the other energy storage devices.

CHAPTER III

REVIEW OF DC/DC CONVERTERS FOR SUPERCAPACITOR INTERFACING

3.1 Introduction

Due to today's technology restrictions supercapacitors have voltages between 2.5 and 2.7 V. Although for low voltage applications such as microprocessors they can be connected directly to the load. The use of dc-dc converters is required to interface these energy storage devices with the vast majority of systems like adjustable speed drives or uninterruptible power supplies systems. There are several suitable topologies to boost the supercapacitor terminal voltage to required voltage levels. These topologies differ in performance, and component count. Therefore it is very important to select the right converter in order to achieve the maximum utilization of the supercapacitor energy thus minimizing loses. A discussion of the main advantages and disadvantages of the suitable topologies is presented in the following points.

3.2. Boost converter

This type of converter is a very well known step-up converter topology and widely used for low power switching power supplies. This topology schematic diagram is shown on figure 11. The operation of this converter can be described as follows, when

the switch Q is in on state, the diode D is reverse biased, thus isolating the output stage of the converter. During this condition the input source supplies energy to the inductor L. When the switch is in off state, the output stage receives energy from the inductor as well as from the input source. This can be seen on figures 11 and 12.

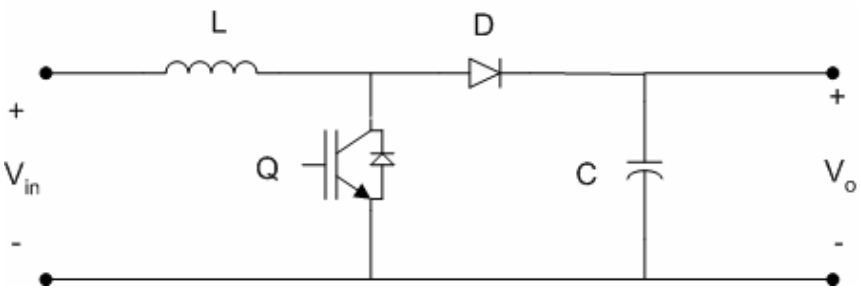

Figure 11 Boost converter topology

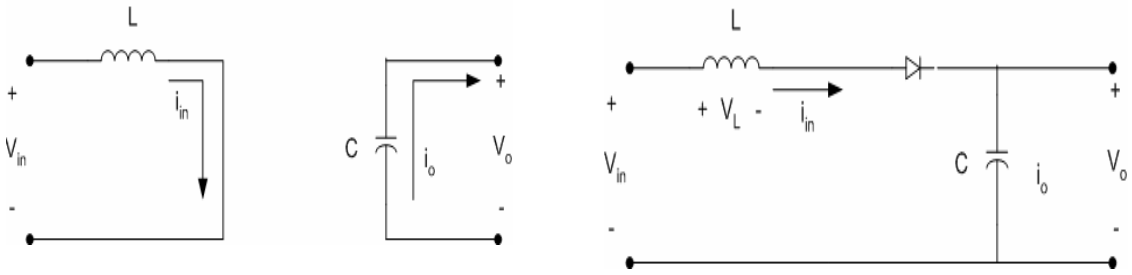

Figure 12 Boost converter operation

The voltage gain of the converter depends on the duty cycle value D, and it can be calculated by means of equation (6)

$$\frac{V_o}{V_{in}} = \frac{1}{1-D} \tag{6}$$

Although from (6) it can be inferred that this converter can have very large voltage gains if a proper duty cycle is selected, a maximum gain of two is achievable in

practical converters. This difference between the ideal voltage gain and the practical voltage gain are due to loses in the inductor, diode and switch. For cases where the output voltage requirements are higher than two or three times the input voltage the use of this topology is not appropriate, because of the reduced efficiency as stated before and the non linear characteristic of the voltage gain of the converter as can be observed on figure 13.

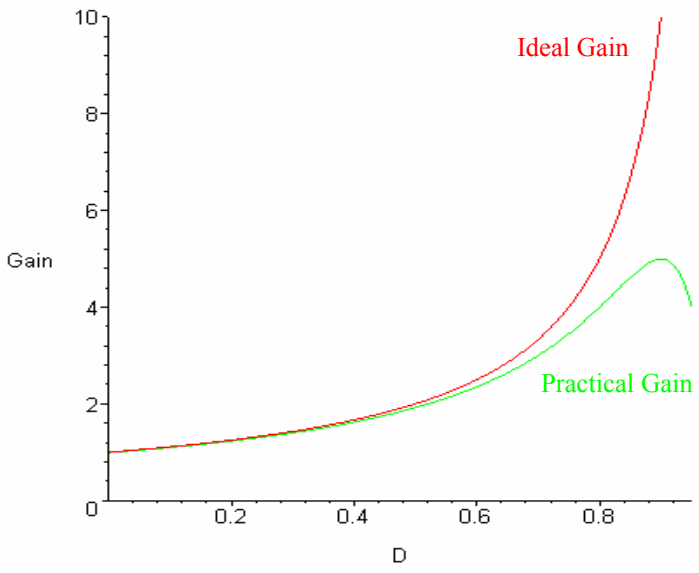

Figure 13 Voltage gain for a boost converter

It is important to consider that this topology does not need transformers and the voltage stress for the switch is relatively low when compared to other dc-dc step-up converter topologies. The use of this topology to step up the voltage supplied by energy storage devices such supercapacitors is feasible when the ratio between the input voltage and the output voltage is no higher than two or three and when no galvanic insulation is required.

3.3. Isolated boost converter

This dc-dc converter topology is an extension of the conventional boost converter. In this case the input and output sides of the converter are isolated by a transformer. The function of the transformer is not only to isolate the grounds of the input and output but also to provide most of the voltage gain of the converter. The circuit schematic of this converter is shown in figure 14. As can be seen from this figure the converter is constituted by two switches two inductors one transformer, snubber capacitor and resistor, four diodes and two output capacitors.

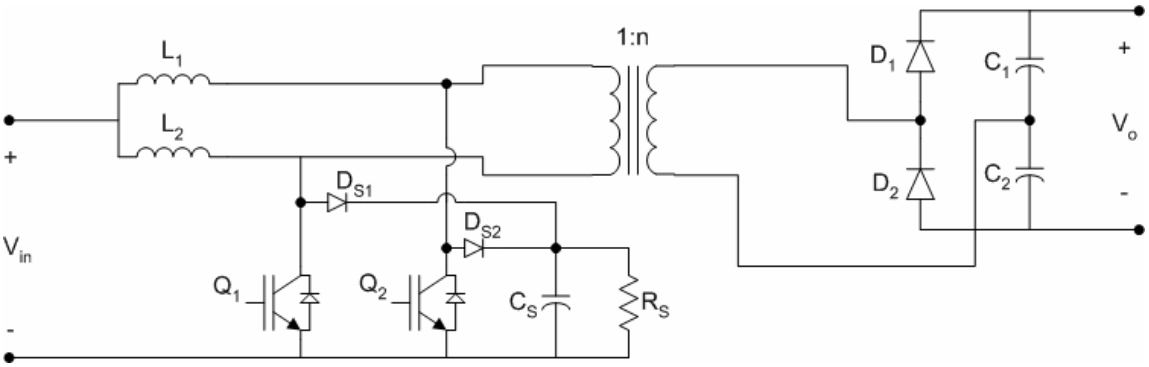

Figure 14 Isolated boost converter topology

Basically in this case two boost converters are connected in parallel. The switches Q_1 and Q_2 operate alternating in order to invert the input dc voltage to get a square wave voltage at the input terminals of the transformer. This voltage is then stepped up by the transformer and then rectified by the half wave rectifier at the secondary part of the circuit. Although most of the voltage gain of the converter is due the transformer the presence of the input inductors L1 and L2 produce a small gain in the same manner as in a boost converter. Also these two inductors allow the converter to

work in continuous conduction, which reduces the input current peak value. This makes this converter suitable for high power applications.

It is obvious that this topology has a much higher component count that the previous one, but has the advantage of being suitable for high power applications and the voltage gain characteristic is better for high gain values than the boost converter. The main problem of this topology is the high switch stress which can be about 4 times the in put voltage of the converter.

3.4. Push-pull converter

Figure 15 shows the circuit schematic for a push–pull dc-dc converter. In this converter the two switches operate to invert the input dc voltage to get a square wave shaped ac voltage. This square wave is then fed to the high frequency transformer which then steps-up the voltage. Finally this voltage is rectified on the output diodes to get a dc output.

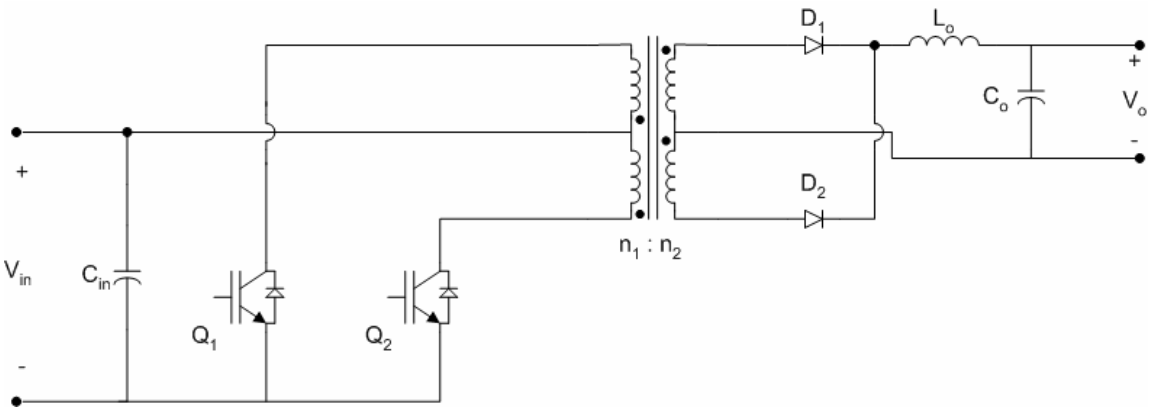

Figure 15 Push-pull converter topology

The voltage gain of this dc-dc converter is given as a function of the duty cycle of the switches Q_1 and Q_2 and can be calculated using equation (7).

$$\frac{V_o}{V_{in}} = 2\frac{n_1}{n_2} D \tag{7}$$

Where D is the duty ratio of the switches, theoretically the maximum value that this ratio can take is 0.5. But in the practice this value has to be under 0.5 to maintain a small blanking time between the two switches since they can not be on at the same time. In this type of converter due to a slight and unavoidable difference between the switching times of the two switches Q1 and Q2, there is always an imbalance between the peak values of the two switch currents. Also due to its operating characteristic this converter topology operates in the discontinuous conduction mode, and therefore the switch peak current value tends to be high.

Also important to consider is the voltage stress to which the switches Q_1 and Q_2 are subjected can be two times the input voltage for this kind of converter. This is not extremely high when compared to the other converters discussed on the previous points. This problem can cause uneven heating on the two switches and produce extra voltage stress on the switch that has to handle a higher current peak value due to higher di/dt. This problem can be solved modifying the topology to work in current mode. This converter topology is discussed in the following point.

3.5. Current feed push-pull

The current feed push-pull topology is basically the same topology as the voltage feed topology discussed on the previous point. It only differs on the inductor placed on the input side of the converter as can be seen on figure 16. By including this inductor in the topology is possible to operate at duty cycles higher than 50%. When operating at duty cycles higher than 50% the converter operates in continuous conduction mode reducing the peak value of the switches. This because operating at high duty cycle values implies that the two switches are conducting at the same time for some time periods and therefore the current is not cut at any moment.

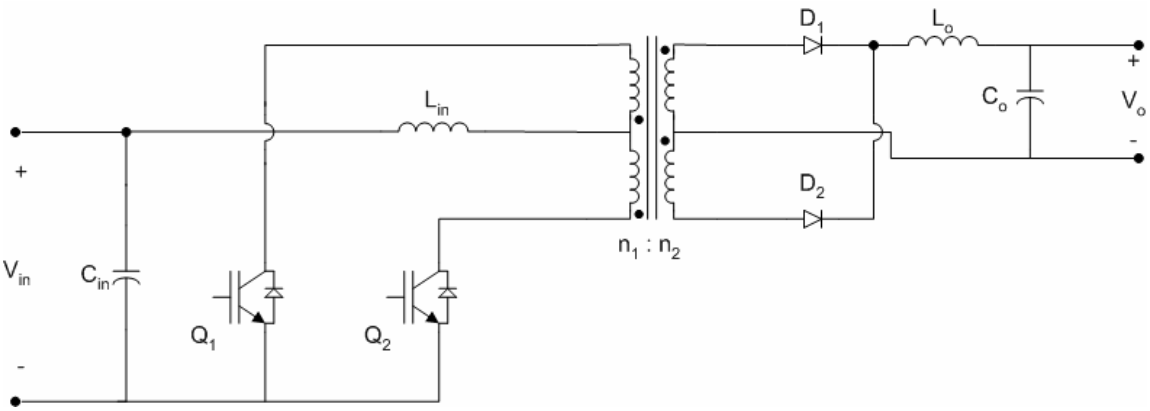

Figure 16 Current feed push-pull topology

When the two switches are on the voltage on the primary half winding of the transformer becomes zero. The input current builds up linearly and energy is stored in the input inductor. When only one of the two switches is conducting, the input voltage and the stored energy in the input inductor supply the output stage of the converter. Therefore this converter operates in a manner similar to a boost converter.

During the continuous current conduction, i.e. duty cycle bigger than 0.5, the voltage gain of the converter can be calculated using (8).

$$\frac{V_o}{V_{in}} = \frac{n_2}{n_1}\frac{1}{2(1-d)} \tag{8}$$

This kind of converter has the disadvantage of having a low power to weight ratio when compared to the converters presented above. Also the voltage stress to the switches is higher tan two times the input voltage when the converter is working below a 0.5 duty cycle. But it has the advantage of reducing the peak value of the switch current for high loads because it works on the continuous conduction mode. This makes this dc-dc converter topology a good option for high power applications.

3.6. Buck-boost converter

This converter topology is slightly more complex than the boost converter since includes one additional switch. But it has the advantage of allowing bidirectional power flow, which means energy can flow from the energy source to the load and back from the load to the energy source. This feature is very convenient for energy storage devices like batteries and supercapacitors, because it allows to recharge the device after each time their energy is used. The operation of this converter is described in the following lines and its schematic is shown in figure 17.

This converter stores energy supplied by the source in the inductor L during the on time of the switch Q_2. When the switch is of the energy of the inductor and the source deliver energy to the load trough the anti parallel diode of the switch Q_1. When an inversion on the power flow direction is required switch Q1 is set on “on” state and

current will flow from the load to the energy source, because the load voltage is always higher than the input voltage.

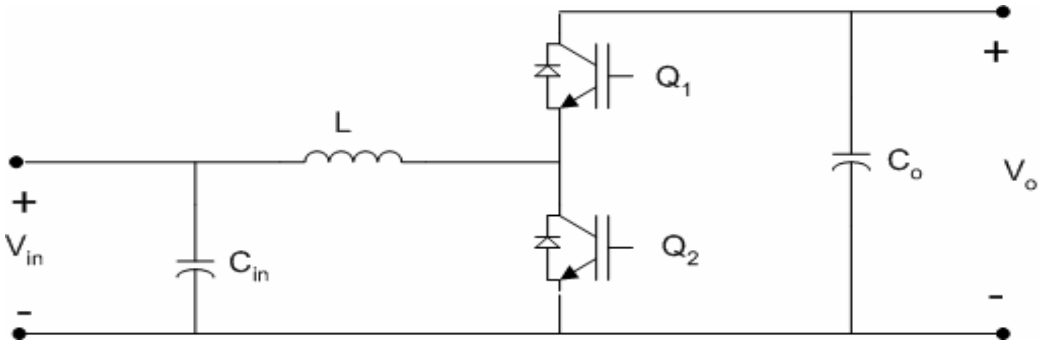

Figure 17 Buck-boost topology

The voltage gain of the converter in terms of the duty cycle of the switches can be calculated using equation (9)

$$\frac{V_o}{V_{in}} = \frac{D}{1 - D} \tag{9}$$

As with the boost converter this topology can only be used when the required voltage gain does not exceed two or three times the input voltage. Thus a buck-boost converter can only be used for low voltage applications or cascades with other dc-dc converter.

Also important to consider as, in the rest of the topologies, is the voltage stress applied to the switches Q_1 and Q_2. In this topology the voltage stress on the switches is given by (10), where V_o it the output voltage and V_m is the peak input voltage to the converter.

$$\text{Voltage stress} = V_o + V_m \tag{10}$$

3.7. Comparison between topologies

Often, the largest cost in a converter is the cost of the semiconductor devices. Also, the conduction and switching losses associated with the semiconductor devices often dominate the total converter losses. Thereby evaluating semiconductor switch utilization is a good tool to compare different converter topologies. So it is useful to compare the totals active stress and active switch utilization of different converter topologies. If a converter topology contains k active semiconductor devices, the total switch stress S can be defined by (11).

$$S = \sum_{j=1}^{k} V_j I_j \tag{11}$$

Where V_j is the peak voltage applied to the j^{th} semiconductor device, and I_j is the rms current applied to the j^{th} switch. If the converter output power is P_{Load}, then the active switch utilization U can be defined by:

$$U = \frac{P_{Load}}{S} \tag{12}$$

The switch utilization is less than one for transformer isolated converters, and is a quantity depending on the duty cycle. A comparison between the converter topologies discussed in previous points is shown in Table 3 below.

Table 3 Switch utilization comparison

Converter	U(D)	Max U(D)	D for max U(D)
Boost	$\frac{(1+D)}{\sqrt{D}}$	∞	0
Isolated boost	$\frac{(1+D)}{2\sqrt{1+D}}$	0.5	0
Push-pull	$\frac{\sqrt{D}}{2\sqrt{2}}$	0.353	1
Current fed push-pull	$\frac{(1+D)}{2\sqrt{1+D}}$	0.5	0
Buck-boost	$(1+D)\sqrt{D}$	0.385	$1/3$

From Table 3 it can be seen that the boost converter switch utilization is greater than one for duty cycles bigger than 0.382, and approaches to infinity as D tends to zero. The reason for this is that, at D=0, the switch is always at its OFF state and hence its rms current is zero. But at D=0 the output voltage is equal to the input voltage, therefore the converter output power is nonzero.

Also from Table 3 it is possible to see that the incorporation of an isolation transformer results in a reduced switch utilization. Therefore this type of converters should be designed to operate preferably at a duty cycle as high as possible.

Finally from the previous table it is possible to see that the buck-boost topology has lower switch utilization than the boost converter; however, isolation can be obtained with no additional penalty in switch stress.

3.8. Conclusion

There is no ultimate converter perfectly suited for all applications perfectly suited for all possible applications. For a given application, with given specifications, trade studies should be performed to select a converter topology. Several approaches that meet the specifications should be considered, and for each approach important quantities such as worst case semiconductor device rms current, size, component count, etc. should be computed. This type of quantitative comparison can lead to selection of the best approach.

CHAPTER IV

USE OF SUPERCAPACITORS AS BACKUP ENERGY TO PROVIDE RIDE THROUGH

4.1. Introduction

Voltage sags are the reduction of the voltage magnitude at the customer terminals, which can have a duration ranging between one cycle and few seconds. This phenomenon is caused by events such as motor starting, fast reclosing of circuit breakers, short circuits, etc. Voltage sags normally do not cause damage to the equipment but they can disrupt the operation of sensitive electronic loads such as the control boards of adjustable speed drives, having the effect of making their protections trip. A sever sag occurrence can be defined as one where the voltage magnitude falls below 85% of its rated value. According to national power quality surveys, voltage sags are the main cause of disturbances in electric distribution systems. These surveys also report that 68% of the disturbances are voltage sags and they are the only cause of production loss. These loses are caused by voltage sags of 13% of the rated voltage and with a duration of more than 8.3 msec. (half a cycle). In textile and paper mills brief voltage sags may potentially cause an ASD to introduce speed fluctuations which can damage the final product. Furthermore short voltage sags can produce a momentary dc-link voltage drop which can trigger the protection circuitry. This kind of nuisance tripping of an adjustable speed drive used on a continuous process can be costly.

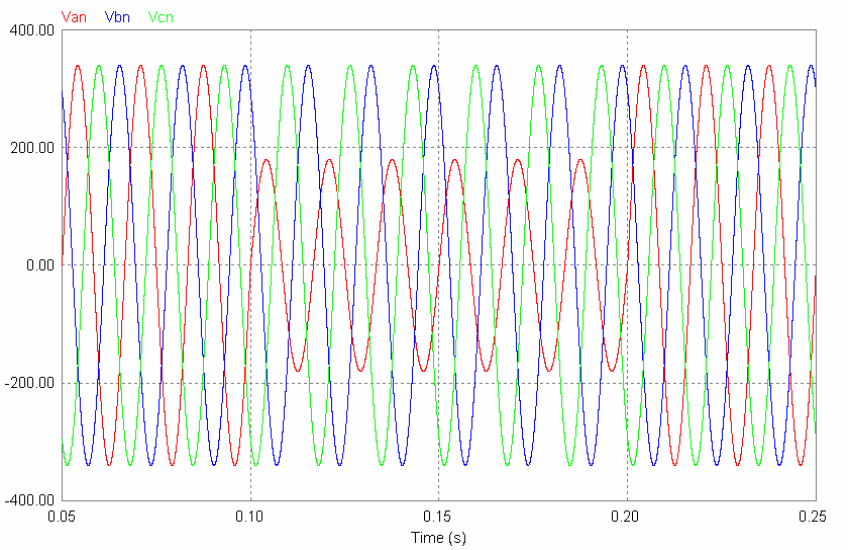

Figure 18 Single phase 50% voltage sag

In Figure 18 a typical single phase voltage sag is shown. In this case the voltage drop in one phase is 50 % of the nominal voltage, and it last for 100 μsec. The effect of this disturbance can be seen in the figure 19. This reduction in the dc link voltage can cause the dc link under voltage protection to trip. To compensate the voltage sag effects in the dc link of the ASD a new compensation scheme is proposed combining an isolated boost converter and a super capacitor. This scheme is capable of compensating deep voltage sags as well as short voltage interruptions. The proposed topology to compensate the voltage sag using supercapacitors is shown in figure 20.

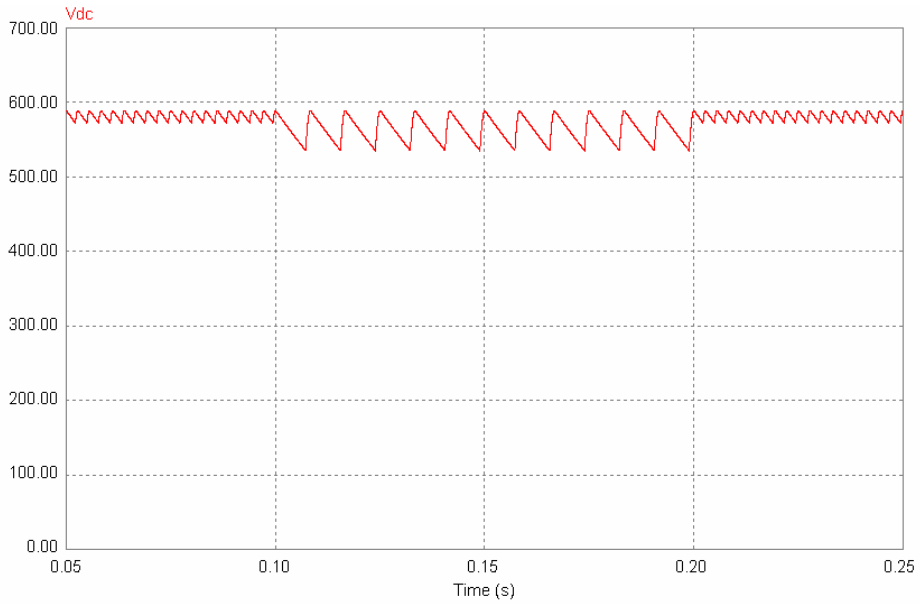

Figure 19 DC link voltage under a single phase 50% voltage sag

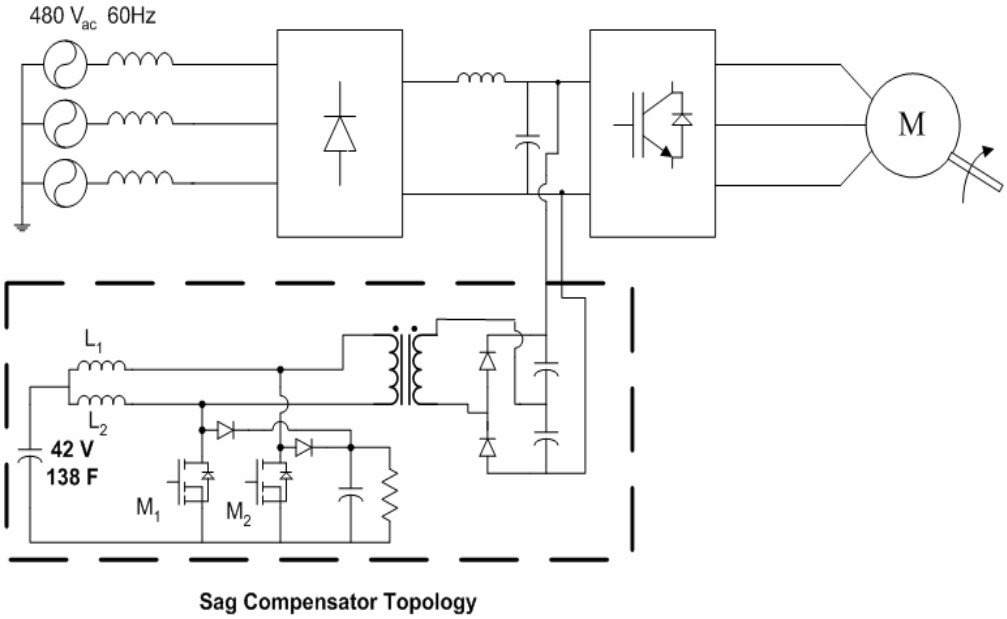

Figure 20 Proposed compensator topology

4.2. Advantage of using supercapacitors as backup energy storage

Power quality applications require instantaneous reliable ride-through power. Using traditional lead-acid batteries for such rapid, deep-cycle electric power demands is harmful to batteries. Also due to the higher ESR of the traditional batteries their use in this kind of application produces higher voltage drops on their terminal voltage and extra losses due to the pulsating characteristic of the load current. In order to ensure constant readiness, using batteries this application will require significant maintenance and high replacement costs. On the other hand, the use of super-capacitors offers significant advantages over the use of batteries. The initial cost per kwh of the super-capacitors commercially available today is higher than conventional batteries, but since they offer higher charge-discharge cycles, and therefore they have a longer life span, and lower maintenance costs they still a good alternative. As discussed in Chapter II the power density of the super-capacitors is much higher than that from the traditional lead acid batteries. This means that Supercapacitors are more suitable for short term applications such as the proposed in this paper.

Recalling from Chapter II the main advantages of the super-capacitors when compared to traditional batteries used in power quality applications can be resumed as listed in the following points:

- Energy densities 100 times greater than conventional capacitors.
- Power densities 10 times greater than batteries.
- Specific energy range of 1.12-2.48 Wh/kg.
- Charge and discharge times of fractions of a second to several minutes
- Rated capacitance value ranging from 0.043-2700 F.
- Nominal voltage ranging from 2.3 – 300 V.
- Rated current ranging from 3 – 600 A.
- Power ranges 5 – 100 kW.
- Cycle life greater than 100000 charge/discharge cycles
- Operating temperature ranging -20 ^{o}C to 55 ^{o}C.
- Modular and stackable.

The above shown set of characteristics makes of the super-capacitors a good option to be used in power quality applications. In ride-through applications, super-capacitors are capable of a quick discharge, due its extremely low ESR's, hence suitable for transient compensation of voltage sags and short voltage interruptions.

4.3. Proposed ride through topology using supercapacitors

The proposed compensator scheme using Supercapacitors is shown in figure 20. It is constituted by a supercapacitor and an isolated boost converter. The operation of the sag compensator scheme is enabled when the magnitude of the voltage sag is bigger than

the threshold value set in the control block of the compensator, normally 10% sag, or when there is a short term voltage interruption. Under this condition the voltage provided by the super-capacitor is then boosted by the dc-dc converter to the dc link voltage level of the ASD system. A block diagram of the control circuit is shown on Figure 21. The time that the module can compensate the voltage disruption depends on the amount of energy stored in the super capacitor and the load being supplied by the ASD. From chapter II the amount of energy stored in the super capacitor is given by the following equation

$$E = \frac{1}{2} CV^2 \tag{13}$$

Where C is the capacitance of the super-capacitor and V is the capacitor terminal voltage. The time that the super capacitor can provide compensation can be calculated using equation (14) which can be derived from equation (13).

$$t = \frac{1}{2} \frac{C}{W} (V_o - V_f)^2 \tag{14}$$

Where t is the total time that the module can compensate, C is the super-capacitor capacitance, V_o and V_f are the initial and final terminal voltage of the capacitor, and W is the required load to be compensated. For example using a 130F capacitor charged at 50 V and considering that the capacitor is discharged when its terminal voltage is 70% of the nominal voltage. Assuming that a momentary voltage interruption on the supply voltage of an ASD is feeding a 20kW load, the total time that the module can

compensate the momentary voltage interruption is 0.731 sec., approximately 45 cycles. The equivalent circuit of the module for this operating condition is in Figure 22. The adequate capacitor seizing is discussed on the following point.

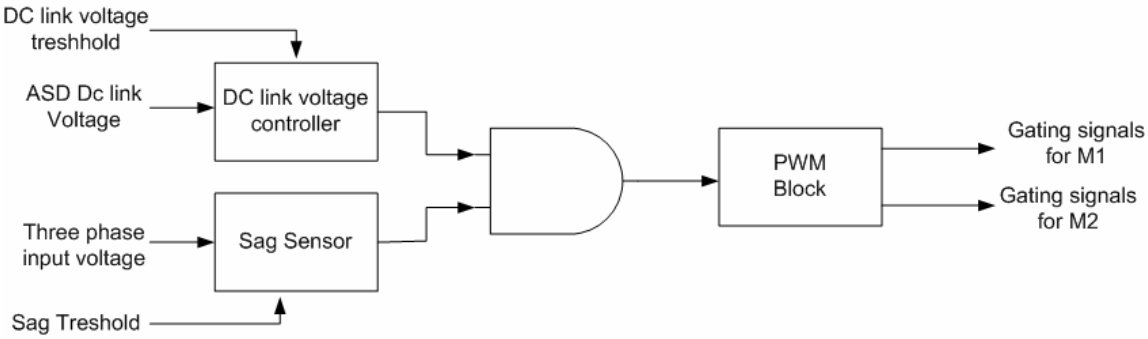

Figure 21 Control circuit Block diagram

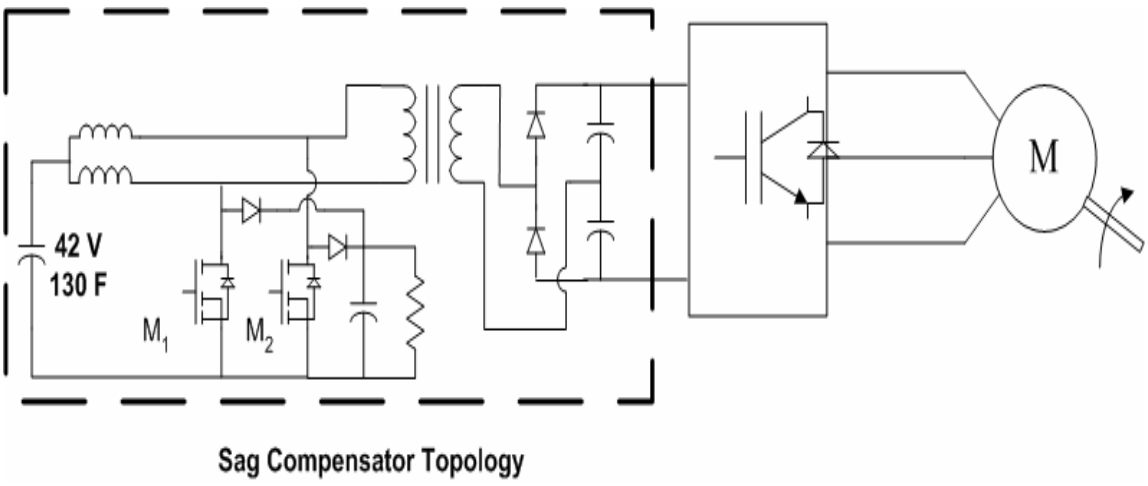

Figure 22 Compensator circuit for deep sags and momentary voltage interruptions

4.4. Design example

Currently super-capacitors are available in 2.5 V units and various capacitance values ranging from 1-5000F. In the design of the converter it is assumed that the super-capacitor bank is constituted by 18 cells and therefore its nominal terminal voltage is 42V. To design the capacitance required to compensate the sags, first the maximum lapse of time that the compensator is going to be capable of supplying energy to the system needs to be defined; in this case 0.5 sec is chosen. The circuit is going to be capable of provide compensation for a short voltage interruption 300 cycles long. Considering that the nominal load of the ASD is 20 kW, the capacitor is discharged when it reaches 0.7% of its nominal voltage, and that the super capacitor is going to provide the energy required to compensate short voltage interruptions (i.e. the worst condition). Using equation (14), which can be written in the form shown in (15), we obtain that a 138F capacitor is required. Since the bank is composed of 18 cells, the required capacitance of each individual capacitor in the bank is 2600 F.

$$C = \frac{2tW}{(V_o - V_f)^2} \tag{15}$$

4.5. Simulation results

The simulated system is a 480 V line to line adjustable speed drive feeding a 20 kW motor load. The parameter values used for the converter are then calculated in the previous point. Connected to the dc link of the ASD is the proposed compensator topology as seen in the figure 20. And the switching frequency of the dc-dc converter is

100 kHz. The first simulated condition corresponds to the ASD system feeding the motor load subjected to a 48% single phase voltage sag. This can be seen in figure 23. The DC link voltage drops more than 50 V during the duration of the voltage sag.

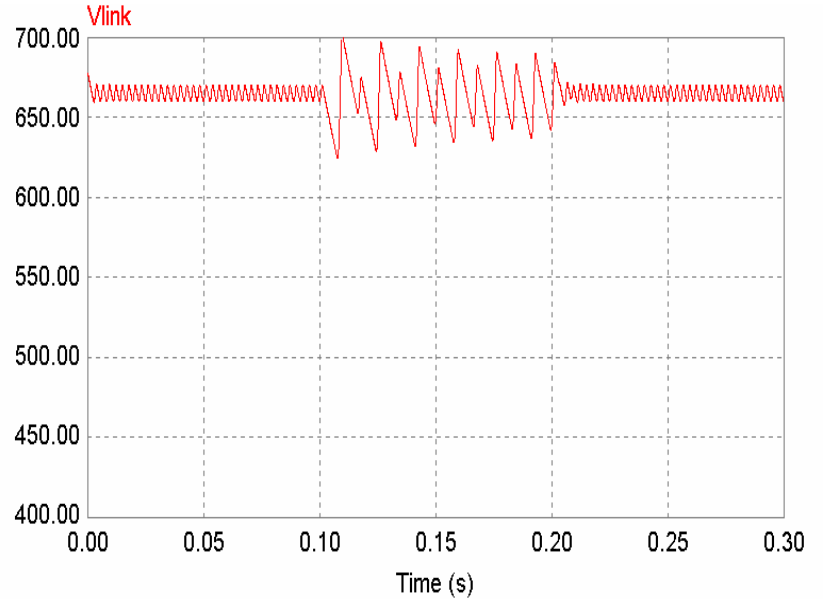

Figure 23 dc link voltage during a 48 % voltage sag without compensation

Figure 24 shows the dc link voltage when the ASD system is subjected to the same conditions and the compensator module is working. The voltage is maintained constant during the transient as seen below.

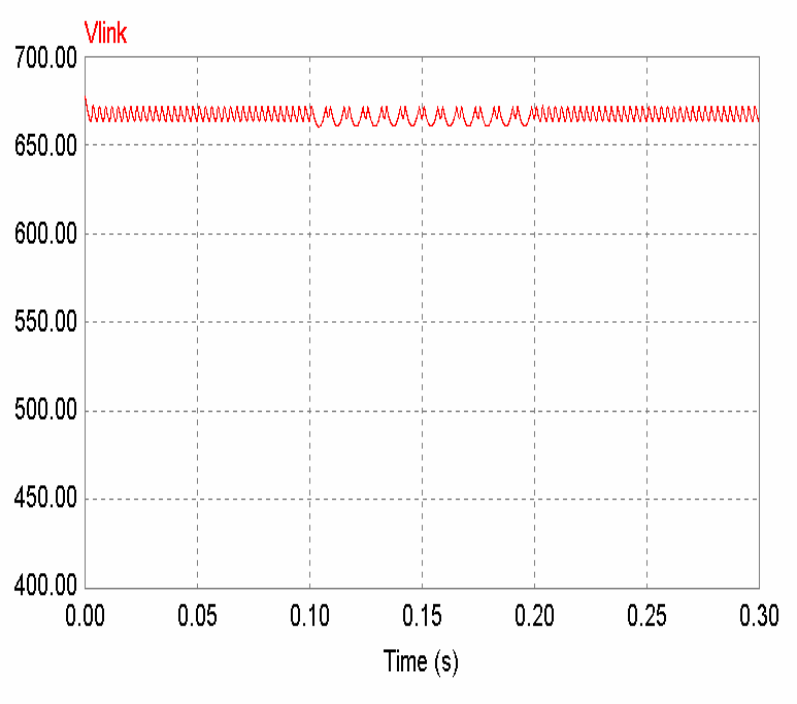

Figure 24 dc link voltage for a 48 % voltage sag with the proposed module

The next simulated situation corresponds to a momentary voltage interruption in the three phases. The duration of the transient is 100 msec. From figure 25 it can be observed that the magnitude of the dc link voltage drops 120 V during the duration of the transient. And after the transient, due to the rapid re-charge of the dc link capacitors, a 350 V over voltage is generated.

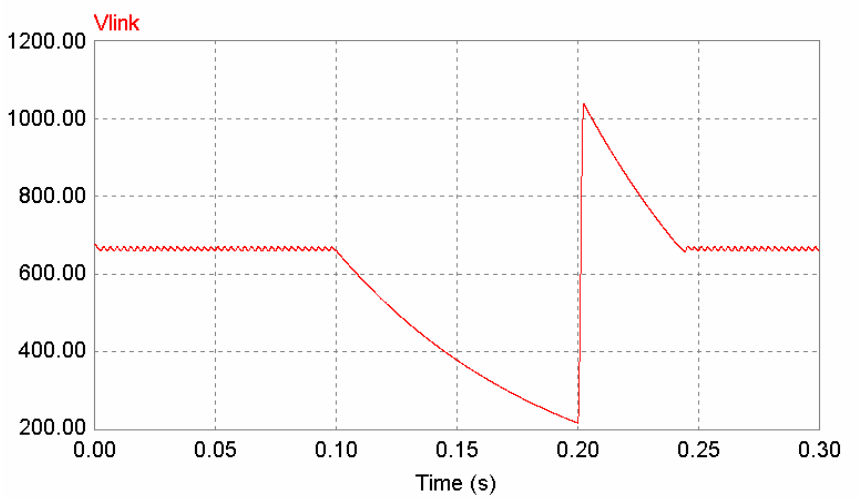

Figure 25 dc link voltage for a momentary voltage interruption without the compensating module

The result for the same condition using the proposed compensator module is shown in figure 26 below. The dc link voltage is kept constant during the transient, avoiding the voltage drop during the interruption and the over voltage generated after the transient ended.

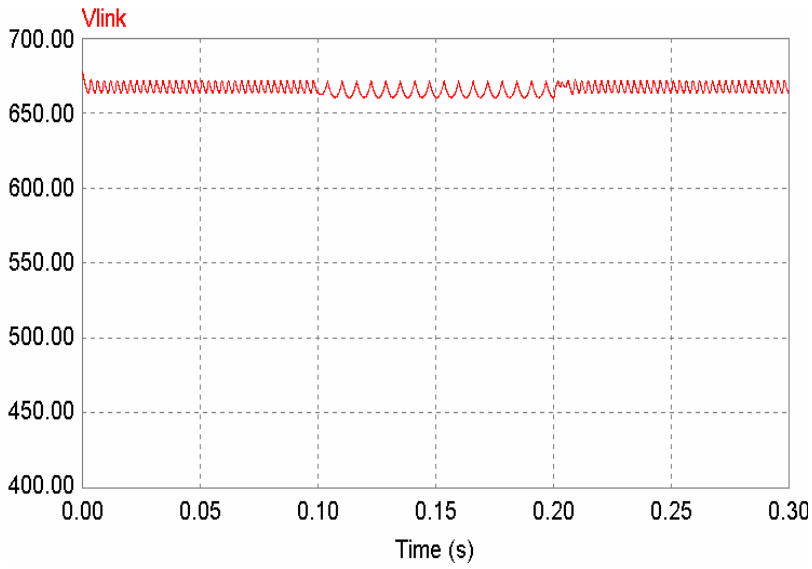

Figure 26 dc link voltage for a 100ms voltage interruption with the module

4.6. Experimental results

The proposed compensator topology was implemented in an experimental prototype, and subjected to single phase and three phase voltage sags, where the voltage drops ranged from 70% to 40%. The response of the compensator is shown in the following figures.

Figure 27 shows the line to line input voltages of the ASD system and the dc link voltage when the system is subjected to a 0.5 sec 3 phase 40% sag, and the compensator system is not connected. As it can be observed in this figure the dc link voltage drops from 130V to 70V during the duration of the sag. The result when the compensator is connected is shown in figure 28. In this case the converter is capable of supplying the energy required to maintain the dc link voltage constant during the duration of the sag. The current supplied by the converter during the sag is shown in figure 29 (5A/div). The transient response of the supercapacitor is fast enough to supply the current required by the ASD during the sag as seen in the figure 29.

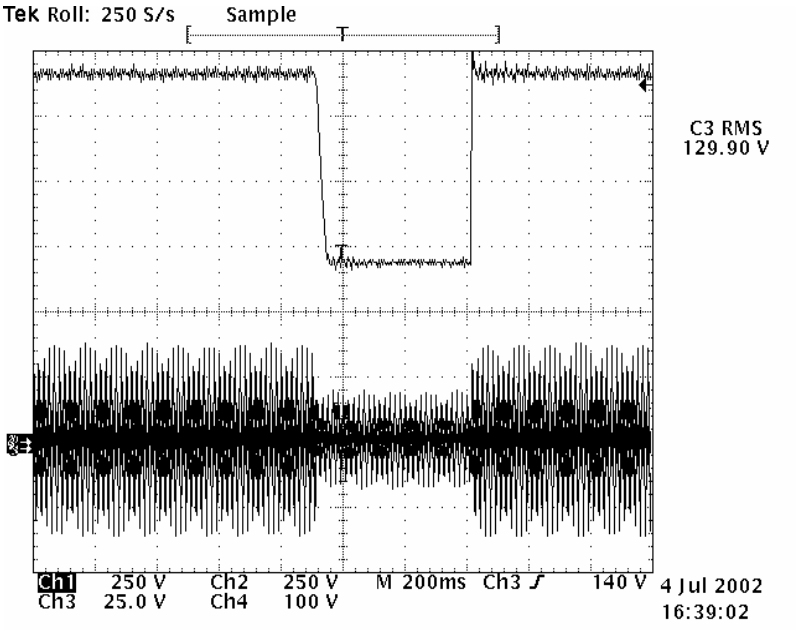

Figure 27 dc link voltage during a 3 phase 50% sag without the converter

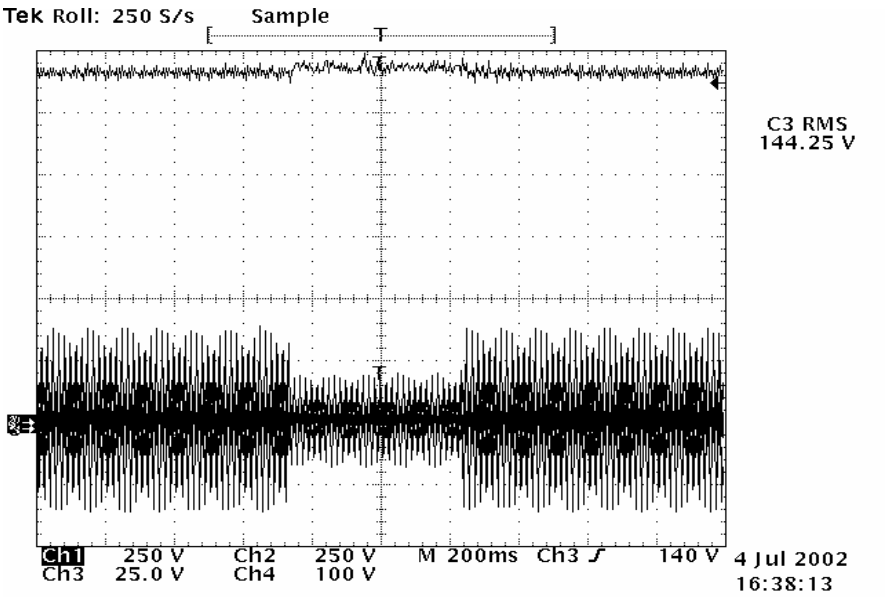

Figure 28 dc link voltage during a 3 phase 50% voltage sag with the converter

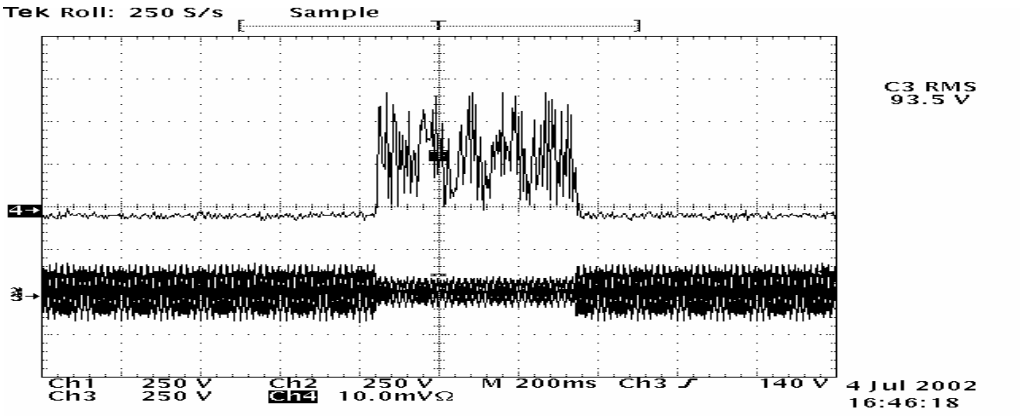

Figure 29 Current supplied by the supercapacitor during the duration of the voltage sag

Figures 30 to 32 show the results for the system subjected to a 0.5 sec three phase short term voltage interruption. In figure 30 the dc link voltage descends to almost 0 volts during the voltage interruption. When the compensator converter is connected the dc link voltage is kept constant by the energy supplied by the supercapacitor as seen in figure 31. Figure 32 shows the current supplied by the supercapacitor during the compensation time (5A/div).

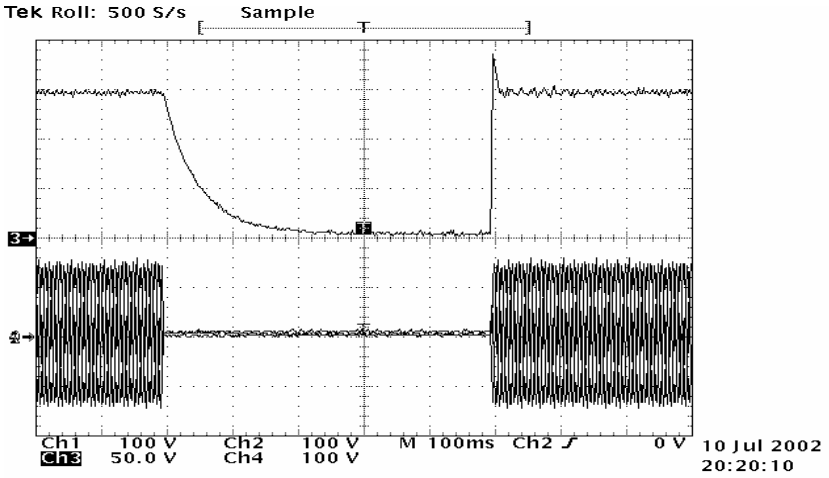

Figure 30 dc link voltage for a 0.5 sec 3 phase voltage interruption without the compensator

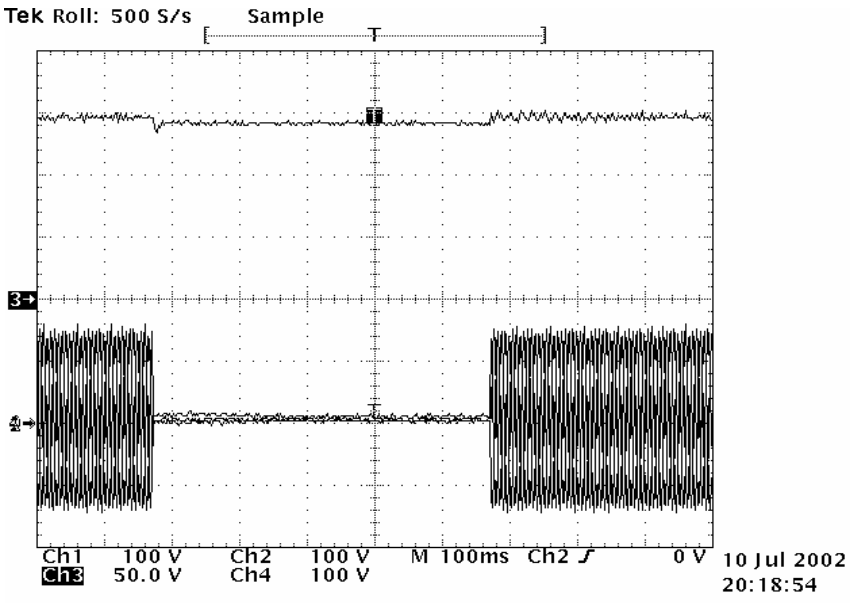

Figure 31 dc link voltage for a 0.5 sec 3 phase voltage interruption with the compensator

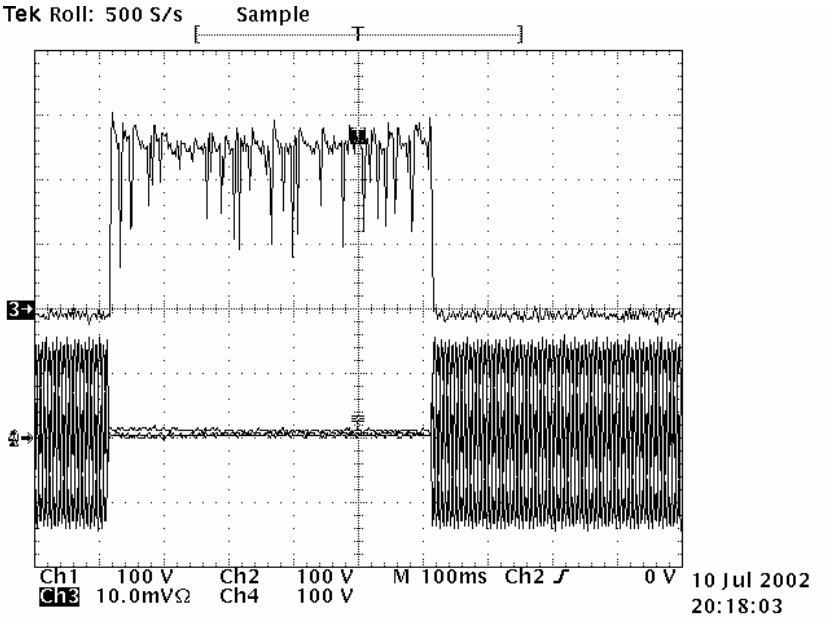

Figure 32 Current supplied by the supercapacitor to the dc-dc converter during the short voltage interruption

4.7. Conclusions

In this chapter the advantages between the use of Supercapacitors and traditional lead-acid batteries to provide ride through were presented and discussed. From this discussion it is clear that Super-capacitors, due to high power density and low ESR, are a very convenient energy storage component to be used in power quality applications. A sag compensator topology using supercapacitors is developed and tested in this chapter.

This compensator topology is capable of providing ride through for deep voltage sags as well as short voltage interruptions. All this, while maintaining the dc link voltage level constant during the duration of the transient disturbance. The available compensation time of the compensator depends on the amount of energy stored in the supercapacitor and the current being drawn by the load. Therefore is important to calculate the roper capacitor size depending on these parameters. For this reason a simple design procedure for the capacitor size is presented. The effectiveness of the proposed ride through topology is shown by means of simulations and experimental results obtained on a laboratory prototype. From these results is clear that the supercapacitor dynamic response is fast enough to respond to the load transient requirements and avoid the effects of the voltage sags on the adjustable speed drive.

CHAPTER V

USE OF SUPERCAPACITORS TO EXTEND BATTERY RUN-TIME IN MOBILE DEVICES

5.1. Introduction

Battery run-time in a mobile device defines the span of time that the device can run from the energy stored in its batteries. In an ideal world, mobile PCs would run all day, allowing them to cut the AC power cord, thus freeing the user to access information wherever they choose without scrambling for electrical outlets. An increase in the run-time can be obtained by having multiple batteries or increasing their rated capacity; with the obvious draw back of increasing the size, weight and maintenance costs of the system. A typical laptop battery is composed by Li-Ion cells with a rated capacity of 4 Ah. Although considerable advances in the Li-Ion battery technology are not keeping up with emerging notebook usage models including digital entertainment, multimedia and wireless connectivity. The expanded usage demands higher power and currents with higher slew rate. The utilization of Supercapacitors to increase the run-time is examined in detail in this paper. Supercapacitors with low equivalent series resistance (ESR) are an emerging technology [6, 16, and 17]. These types of capacitors do not possess the energy density of a conventional battery, however, their power density is several times higher (Table 4) than that of the conventional battery. These features make Supercapacitors a good candidate for improving the performance of battery based applications, where the

battery supplies the energy and the Supercapacitor delivers short-term power. Benefits of this combination include: Enhanced peak power performance, run-time extension, and reduction in internal losses.

Present day Supercapacitors are available with capacitance values ranging from 1F to 5000F, power densities of 4300 W/kg and maximum energy storage of 8125 J [13-15]. Supercapacitor ESR values range from 0.3 mΩ to 130mΩ, five times smaller than a conventional battery ESR. Therefore combining batteries and Supercapacitors is definitely advantageous in supplying pulsating loads. In this paper three approaches for combining the battery and Supercapacitors are proposed. In the first approach, a direct connection of the Supercapacitors to the battery terminals is explored (Figure. 38). This requires the voltage rating of the Supercapacitors to match the battery, thus several supercapacitor cells connected in series are needed. In the second approach, an inductor connected in series with the battery and a supercapacitor in parallel are used to improve the current distribution between capacitor and the battery (Figure. 36). The third approach uses a DC-DC converter along with Supercapacitors to interface with the battery (Figure. 37). This scheme has the advantage of utilizing lower voltage Supercapacitors which are interfaced to standard battery packs by a dc-dc converter. The performance of these schemes are evaluated and discussed in this paper for a battery powered mobile device.

5.2. Battery / supercapacitor technology & circuit model development

Batteries are some of the most cost-efficient energy storages available today, where the energy is stored electrochemically. They are made of several low voltage cells connected in series to achieve the desired terminal voltage. The advantages of the batteries are high energy density and low initial cost. However, they exhibit lower power density, larger size/weight, low cycle life and relative high ESR, when compared to conventional capacitors or Supercapacitors. Further, batteries are not capable of supplying efficiently pulsating loads, which deep discharges [19-20]. The most relevant battery parameters are shown in Table 4.

Table 4 Comparison between different energy storage devices

Energy Source	Energy [kJ]	Energy density [W/h]	Power Density [W/kg]	Price [US$]	Volume [cm3]	Weight [kg]	ESR [mΩ]	US$/ Wh
Supercapacitors by Maxwell [13]	0.031	0.04	1500	10	3.8	0.0064	130	250
Supercapacitors by Siemens Matsuchita [14]	0.021	0.006	769	-	3.1	0.006	125	-
Supercapacitors by EPCOS [21]	0.031	0.04	1900	-	3.2	0.0064	110	-
4 Ah Li-ion Battery	204.5	56.8	<1000	150	24.6	0.39	500	2.64

On the other hand Supercapacitors offer power densities 10 times greater than batteries with considerable lower ESR values. Table 4 illustrates some important parameters associated with the present day commercially available Supercapacitors. [13, 14, 21].

5.2.1. Equivalent circuit of the battery-supercapacitor combination

Figure 33 shows a simplified equivalent circuit model of a supercapacitor connected in parallel with a battery. Where V_b is the open circuit voltage and R_b is the equivalent resistance. The supercapacitor model is assumed to be an ideal capacitor in series with its equivalent series resistance R_c. These parameters can be obtained from the manufacturer data sheets or via experimental measurements. The Thevenin equivalent circuit of the battery and the capacitor combination in parallel is given by equations (16) and (17) and is shown in Figure 33.

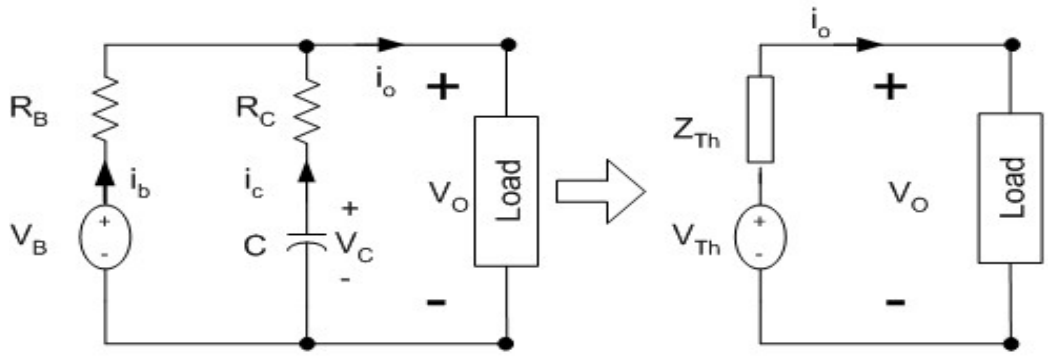

Figure 33 Equivalent circuit of the battery supercapacitor combination

$$Z_{TH}(s) = \frac{R_B R_C s + \frac{R_b}{C}}{(R_B + R_C)s + \frac{1}{C}} \tag{16}$$

$$V_{TH}(s) = V_B \frac{R_C s + \frac{1}{C}}{(R_B + R_C)s + \frac{1}{C}} + V_C \frac{R_B R_C C^2 s^2 + R_B C s}{(R_B R_C + R_C^2)C^2 s^2 + (R_B + 2R_C)Cs + 1} \tag{17}$$

The above equivalent circuit model can be considered to be accurate for 0-1kHz range [17]. From (16) it can be seen that the equivalent impedance of the system is reduced, allowing it to supply higher currents with less voltage ripple.

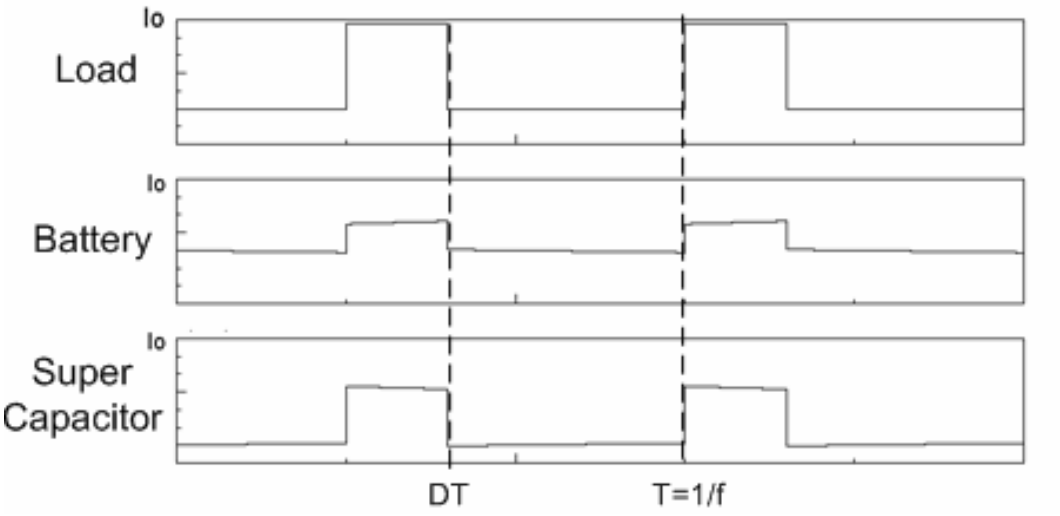

Figure 34 System currents

Figure 34 shows the waveforms for the current supplied by the battery/supercapacitor for a pulsating load of magnitude I_o and frequency f. It is clear from Figure 34 that the battery peak current is reduced due to the presence of the supercapacitor in parallel (whit lower ESR). From Figure 33 we have

$$V_o = V_{th} - Z_{th} * i_o \tag{18}$$

Where io is given by ,

$$i_o = I_o \sum \frac{4}{n\pi} \sin(n\varpi t) \tag{19}$$

Also,

$$i_b = \frac{V_b - V_o}{R_b} \tag{20}$$

From (16) to (20) we have,

$$i_b(t) = I_o \sum_{n=0}^{N-1} [(1 - \frac{R_b}{R_b + R_c} e^{-\frac{(t-nT)}{(R_b+R_c)C}}) H(t-nT) - (1 - \frac{R_b}{R_b + R_c} e^{-\frac{(t-(n+D)T)}{(R_b+R_c)C}}) H(t-(n+D)T)] \quad (21)$$

From Figure 34, it is clear that the battery current reaches its peak value at t = DT, therefore the peak value of the battery current is given by,

$$I_{bpeak} = I_o (1 - \frac{R_b e^{-\frac{DT}{(R_b + R_c)C}}}{R_b + R_c} \frac{1 - e^{\frac{-(1-D)T}{(R_b + R_c)C}}}{1 - e^{\frac{T}{(R_b + R_c)C}}} \quad (22)$$

$$= I_o \frac{1}{p\_enhance}$$

Where *p_enhance* can be defined as the amount by which the battery current is reduced due to the parallel combination of the supercapacitor and the battery. From (22) we have,

$$p\_enhance = \frac{1}{1 - \frac{R_b}{R_b + \frac{R_c}{m}} \frac{e^{-\frac{DT}{(R_b + \frac{R_c}{m})mC}} (1 - e^{-\frac{(1-D)T}{(R_b + \frac{R_c}{m})mC}})}{1 - e^{\frac{T}{(R_b + \frac{R_c}{m})mC}}}} \quad (23)$$

From Figure 33 the internal losses due to the hybrid connection of the battery & supercapacitor ($P_{Loss\text{-}bc}$) is given by,

$$P_{Loss\ ,bc} = R_b I_{b,rms}^2 + R_c I_{c,rms}^2 \quad (24)$$

Where I_b and I_c are the rms values of the battery and supercapacitor respectively (Figure 34). Further, the losses in the battery when the supercapacitors are not connected in parallel can be calculated by,

$$P_{Loss\ -b} = R_b I_o \sqrt{D} \quad (25)$$

It is clear from Figure. 34 and (23),(24) that there is a reduction in the loses within the battery due to the usage of supercapacitors. The reduction in power loss *ΔP is*

$$\Delta P = P_{Loss,b} - P_{Loss,bc} \quad (26)$$

And the normalized power loss can be calculated by,

$$\Delta P_n = \frac{\Delta P}{P_{Loss\ ,b}} \quad (27)$$

The net reduction in the loses in the battery can now be assumed to be available to the load and the resulting run-time extension can be calculated as,

$$\Delta t = \frac{\Delta P}{P_o} \quad (28)$$

Where Po is the output power supplied to the load as is given by,

$$P_o = V_{o,rms}\, I_o \sqrt{D} \tag{29}$$

Therefore, a net reduction in losses due to the connection of Supercapacitors in parallel with the battery is then assumed to result in additional run-time extension.

5.2.2. Equivalent circuit of the battery- supercapacitor-inductor combination

In this approach an inductor L is connected in series with the battery, as shown in Figure 35. The introduction of this inductor into the battery-capacitor system is to soften the current waveform being supplied by the battery and further increase the current redistribution from battery to capacitor.

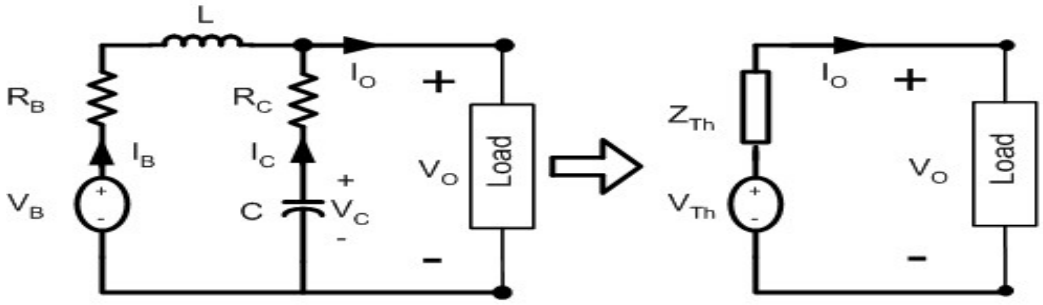

Figure 35 Equivalent circuit of the battery supercapacitor combination

The Thevenin equivalent circuit for this case is described by,

$$Z_{th} = \frac{R_b R_c (\gamma s^2 + \phi s + \alpha)}{(R_b + R_c)(\varepsilon s^2 + s + \beta)} \tag{30}$$

$$V_{TH} = \frac{R_b R_c}{R_b + R_c} \frac{s + \alpha}{\varepsilon s^2 + s + \beta} V_b + \frac{R_b}{R_b + R_c} \frac{s * (\varepsilon s + 1)}{\varepsilon s^2 + s + \beta} V_c \tag{31}$$

Where the factors α, β, γ,ε and ϕ depend on the battery, inductor, and capacitor parameters, and are given by:

$$\alpha = \frac{1}{R_c C} \qquad \gamma = \frac{L}{R_b}$$

$$\beta = \frac{1}{(R_b + R_c)C} \qquad \varepsilon = \frac{L}{Rb + Rc} \qquad \phi = 1 + \frac{L}{R_b + R_c} \tag{32}$$

Using the same approach detailed in 5.2.1, we have that the peak power enhancement can be calculated using the equivalent circuit of Figure 35 and its Thevenin representation. This factor can be calculated by (33). From this equation, and as in the previous case, the peak current supplied by the battery is reduced. This has the effect of reducing the internal loses in the battery. Loses in the system can be calculated by (26) and similarly as in the previous condition the normalized power saving is given by (27). The run-time extension produced by the internal loss reduction can again be calculated based on the power saved using equations (28) and (29).

$$p\_enh = \frac{1}{\frac{R_c}{R_b + R_c}\left(\frac{\alpha e^{-\frac{DT}{2\varepsilon}}}{\beta}\left(-\frac{\sinh\left(\frac{DT\sqrt{1-4\varepsilon\beta}}{2\varepsilon}\right)}{\sqrt{1-4\varepsilon\beta}} - \cosh\left(\frac{DT\sqrt{1-4\varepsilon\beta}}{2\varepsilon}\right) + \alpha\right) + \frac{(2\phi\varepsilon + \gamma\sqrt{1-4\varepsilon\beta} - \gamma)\left(e^{\frac{\sqrt{1-4\varepsilon\beta}-DT}{2\varepsilon}} - 1\right)}{4\varepsilon\sqrt{1-4\varepsilon\beta}} + \frac{(\gamma\sqrt{1-4\varepsilon\beta} - 2\phi\varepsilon + \gamma)\left(e^{-\frac{DT(1+\sqrt{1-4\varepsilon\beta})}{2\varepsilon}} - 1\right)}{4\varepsilon\sqrt{1-4\varepsilon\beta}}\right)} \tag{33}$$

5.3. Approach to improve battery run-time in mobile applications

As discussed in the previous points the connection of a supercapacitor in parallel with the battery has the effect of reducing the peak value of the current supplied by the battery. This has the effect of reducing internal loses in the system and the rms value of the current being supplied by the battery. The power saved by this connection results in additional run-time for the system. To connect the supercapacitor to the battery three methods are proposed. Figure 36 shows the method of direct connection of the supercapacitor to the battery. This supercapacitor connection approach can be divided into two depending on if an inductor is connected in series with the battery or not. The third approach is shown in Figure 37. In this case the supercapacitor is connected to the battery using a dc-dc converter.

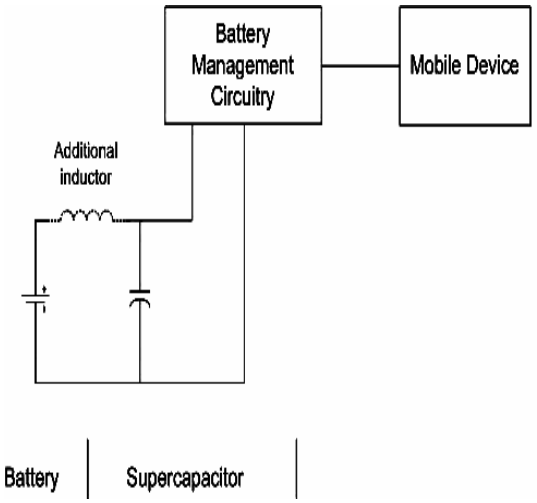

Figure 36 Direct connection of the supercapacitor

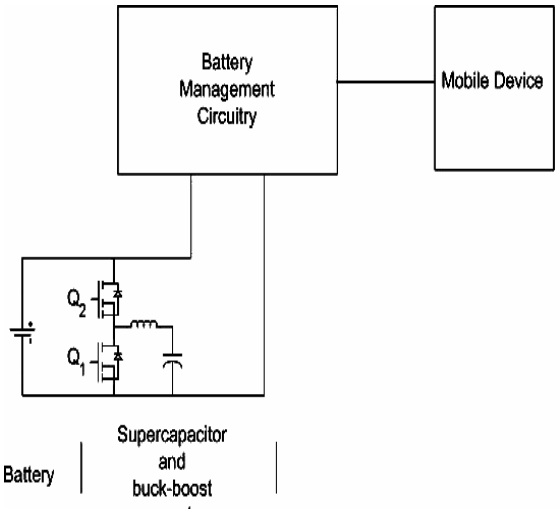

Figure 37 Supercapacitor connection using a dc-dc converter

5.3.1 Direct battery supercapacitor connection

This approach requires the supercapacitor voltage to match the battery voltage. Since the nominal voltage of the supercapacitor cells available today is 2.5 V several capacitors connected in series are needed. For example to connect to a typical notebook battery which has a voltage of 14.2 V it is necessary to connect 6 supercapacitors in series (Figure 38), thus increasing the ESR and cost of the equivalent capacitor.

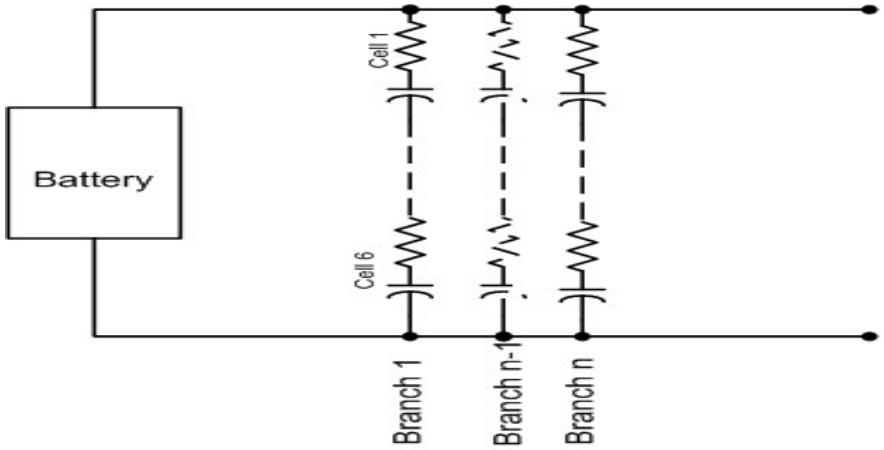

Figure 38 Direct capacitor connection

To analyze the performance of this connection the equations derived in the previous point along with the battery and supercapacitor parameters of Table 4 are used. To match the battery voltage six capacitors are connected in series to form an equivalent supercapacitor of 3F. Figure 39 shows the relative power enhancement as function of frequency and duty cycle. From this figure it can be observed that for pulses of short duration the enhancement in the power delivering capability is higher, and that for frequencies above 2 Hz the power enhancement is independent of the frequency and

depends only on the duty cycle of the pulsating load. This because for high frequency operation the voltage drop due to the discharge of the capacitor is negligible.

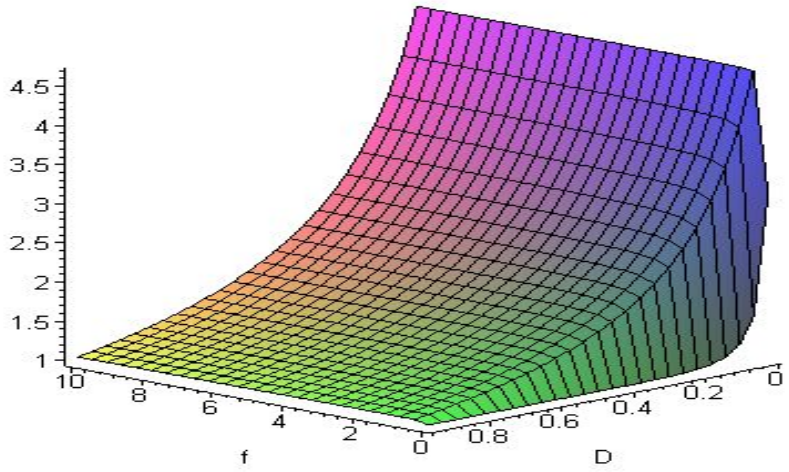

Figure 39 Variation of p_*enhance* (y-axis) of battery supercapacitor hybrid as a function of frequency *f* and duty cycle D

Figures 40a and 40b show the relative power loss reduction in the battery-supercapacitor system calculated from the equations derived in 5.2.1 and using the parameters given in Table 4. From Figure 40a it can be observed that the loss reduction also depends on the duty cycle D of the load. Also the number of capacitor branches connected in parallel with the battery has an effect in the internal loss reduction. The effect of adding multiple capacitor branches in parallel contributes to a reduction in the equivalent ESR and simultaneous reduction in losses. However, adding more than 3 capacitor branches does not seem to yield much loss reduction.

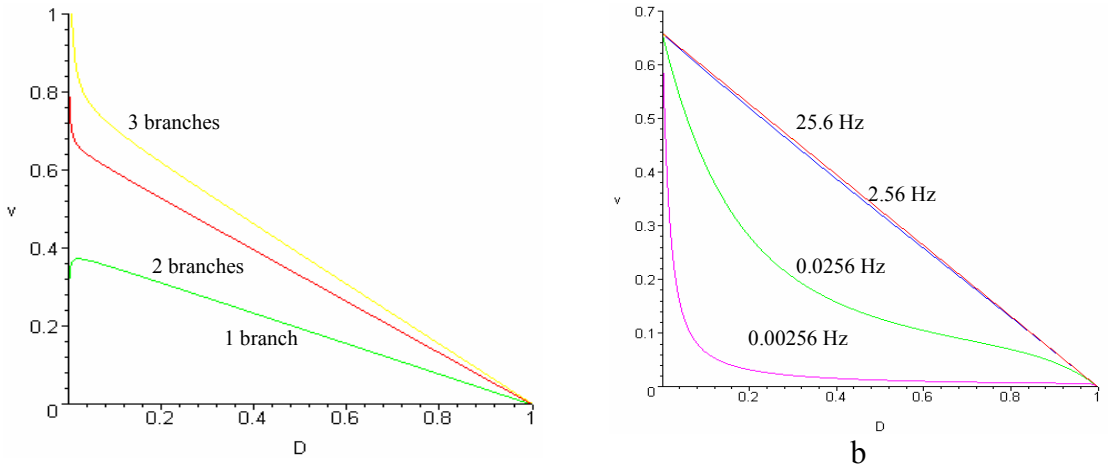

a b

Figure 40 Relative System loss reduction in the battery-supercapacitor connection

Further from Figure. 40b it can be deduced that reduction in $P_{loss\text{-}bc}$ is negligible at very low frequencies and it is almost constant for frequencies above 1 Hz. Based on the internal loss reduction and equations (26) and (27) it is possible to compute the number of capacitor branches needed for a specified run-time extension (Δt). The number of branches M is given by,

$$M := -\frac{dt\ Rc}{Rb\ (dt - dt\ dl\ \sqrt{\mathrm{D}} + dt\ dl\ \mathrm{D}^{(3/2)} - dl\ \sqrt{\mathrm{D}} + dl\ \mathrm{D}^{(3/2)})} \tag{34}$$

Figure 41 shows the number of capacitor branches in parallel needed for different run-time extensions. From this figure it can be seen that from the internal loses reduction point of view a maximum run-time extension of 6.2 % is possible. Additional run-time extension is possible due to the reduction in the battery rms current value. This extra time gained depends of the battery chemical characteristics and can be determined from it discharge characteristics. A typical battery discharge characteristic is shown in Figure

42. As can be seen from this figure reducing the rms current supplied by the battery from its nominal value to 0.9 times its nominal value has a considerable effect in run-time.

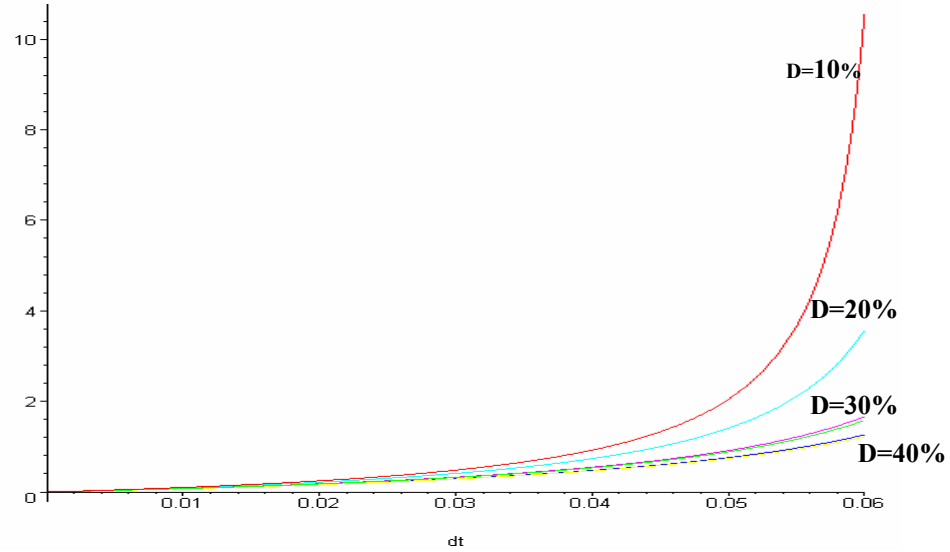

Figure 41 Number of capacitors required as function of relative run-time extension

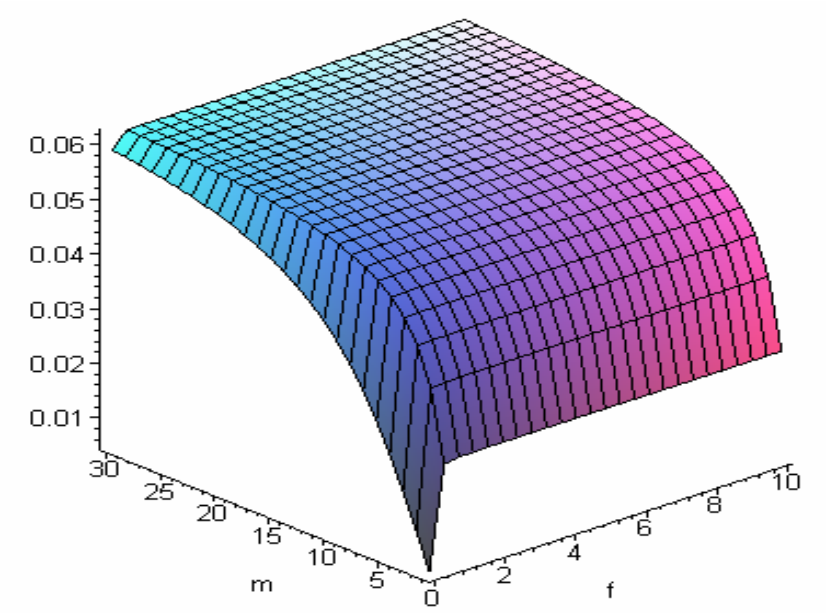

Figure 42 Run-time extension vs. frequency and number of capacitors

Currently supercapacitor cells for low power applications such as the discussed in this point have a relatively high ESR value when compared to the ones used for high power. Currently manufacturers are improving the materials used to construct the supercapacitors cells and therefore their ESR values are expected to drop considerable in the upcoming years. Due to this fact is of interest to evaluate the effect of the ESR reduction on the run-time. Figure 43 shows the run-time extension as a function of the number of supercapacitor branches and capacitor resistance. As can be seen from this figure due to the reduction in the capacitor resistance an extra 1.5% run-time can be expected.

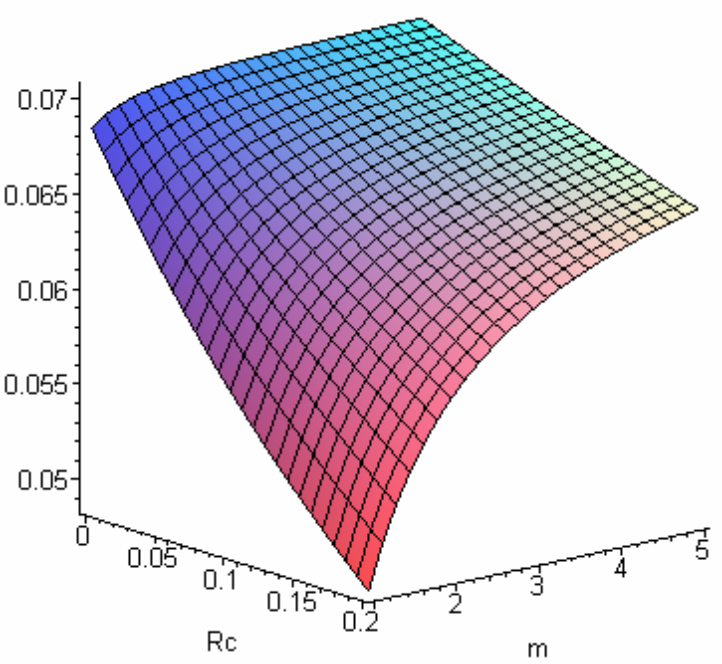

Figure 43 Run-time extension vs. capacitor ESR and number of branches in parallel

Also the reduction in the capacitor ESR has the effect of improving the current being delivered by the battery, since it further reduces its peak and rms values.

5.3.2. Battery-inductor capacitor connection

The performance of this approach is evaluated in this point. For this the equations developed in point 5.2.2 and the battery and capacitor parameters of Table 4 were applied. Since this method also requires the capacitor to be connected directly to the battery, six capacitor cells need to be used. Thus increasing the equivalent capacitor ESR and reducing its equivalent capacitance. Figure 44 shows the resulting power enhancement for different inductor values and number of capacitor branches connected in parallel. From this result it is possible so observe that to get a maximum peak power enhancement a 100mH inductor is needed.

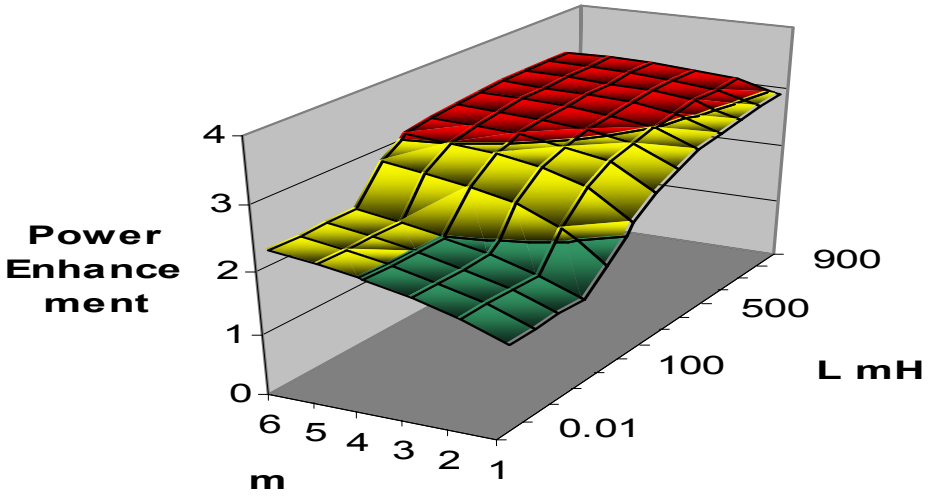

Figure 44 Peak power enhancement vs. inductor value and number of capacitors in parallel

The loses in the battery-inductor-capacitor system can be calculated by means of the equivalent circuit using the same approach as in the previous case. For this it was assumed that the load current is a low frequency pulsating current. The resulting relative

power loss using a 100mH inductor for different frequencies and duty cycles is shown in figure 45.

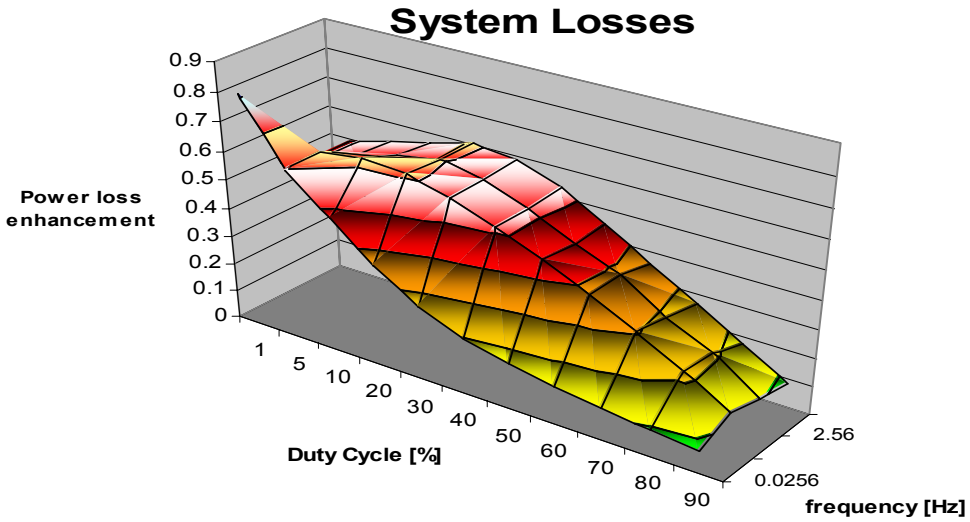

Figure 45 Battery-inductor-capacitor losses

It is possible to see that by adding the inductor and capacitor to the system the losses can be reduced. The loss reduction fluctuates in a range 1-8% depending on the duty cycle of the pulsating current. From the figure is important to note that the highest power loss reduction is achieved for a 30% duty cycle. The extra energy gained by the reduction in the internal loses derives into additional run-time.

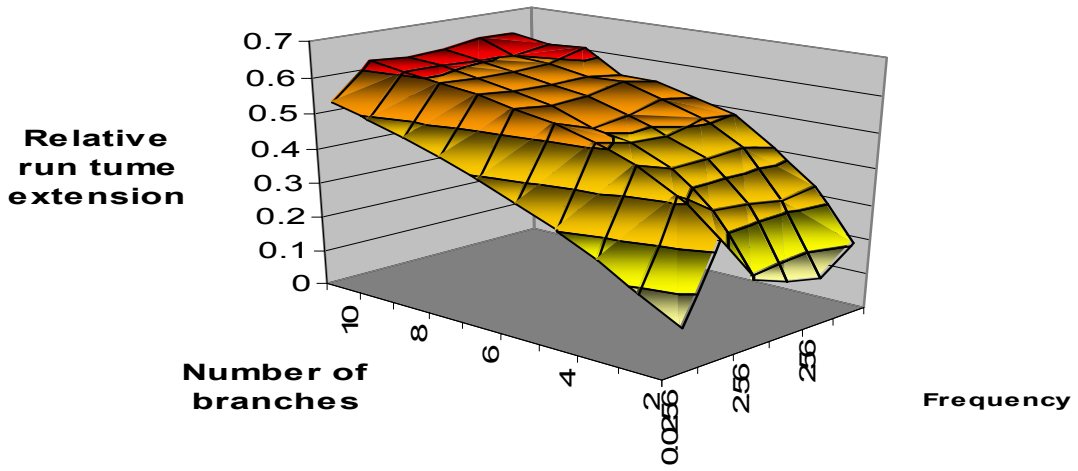

Figure 46 Relative time extension vs. frequency and number of capacitors for a 100mH inductor

Figure 46 shows the run-time extension achieved by the connection of a 100 mH inductor with a pulsating load current with a 30% duty cycle and different number of capacitors in parallel. This figure was obtained calculating loses in the battery supercapacitor system and comparing them with the loses when only a battery is used. From this figure it is possible to see that the maximum run-time extension that can be achieved from system loses point of view is 6.5%.

5.3.3. Use of dc-dc converter

The third supercapacitor connection approach is shown in Figure 37. In this case a supercapacitor bank of lower voltage than the battery nominal voltage is connected via a buck-boost converter. The operation of this topology can be braked down in two stages. The first one is during the charge mode, when switch Q_2 is on. This operation stage can be divided in to two sub states depending on if the load is taking current or not. If the load is not taking current the super capacitor is charged by the battery. In the

alternate case if the load is taking current then the battery voltage drops below the boosted voltage of the supercapacitor because of its internal impedance and the capacitor delivers energy to the load. The second operation mode is during the discharge period, when the switch Q_1 operates boosting the supercapacitor voltage to the battery voltage level. As said before the typical current being taken by a mobile device is a low frequency pulsating current. Therefore during the load operation the dc-dc converter will be alternating from modes 1 and 2 constantly. The performance of this approach is equivalent to the direct capacitor connection approach, shown in Figures 39 to 43. But it has the advantage of requiring less capacitor cells connected in series, therefore reducing the cost of the approach. Also it reduces the rms current delivered by the battery having the effect of increasing the run-time as shown in figure 47 below.

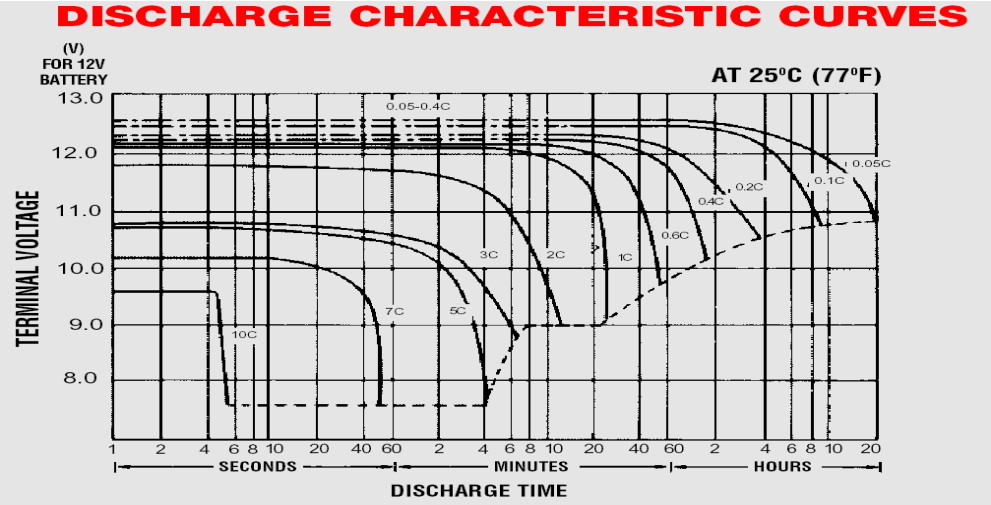

Figure 47 Discharge characteristics typical battery

5.4. Simulation results

A battery powered mobile device was simulated using the equivalent circuits discussed above. The system consists of a 14.2 V battery having an internal resistance of 500 mΩ and a super capacitor bank consisting of an equivalent 3.3 F supercapacitor with an ESR of 390 mΩ. The load connected to the system is drawing 2.4 A peak at 1Hz and 40% duty cycle. The system temperature was assumed to be constant at 25^{o}C. The simulation result can be observed in the next figure. From figure 48 the RMS current being supplied by the battery without the supercapacitor connected to its terminals is 1.5 A and has a peak value of 2.4 A. In the case of the battery and supercapacitor combination the RMS current supplied by the battery is 1.2 A and its peak value is 1.6 A. That means a reduction of a 24% in the RMS current delivered by the battery. This current is much better from the battery point of view and will change the discharge curve of the battery, were the curve that has to be used to predict the battery run-time is 0.76C instead of 1C. In the case of the voltage ripple caused by the voltage drop in the ESR of the battery, the connection of the supercapacitor across the battery terminals reduces this drop by reducing the value of the peak current. This can be seen in figure 49.

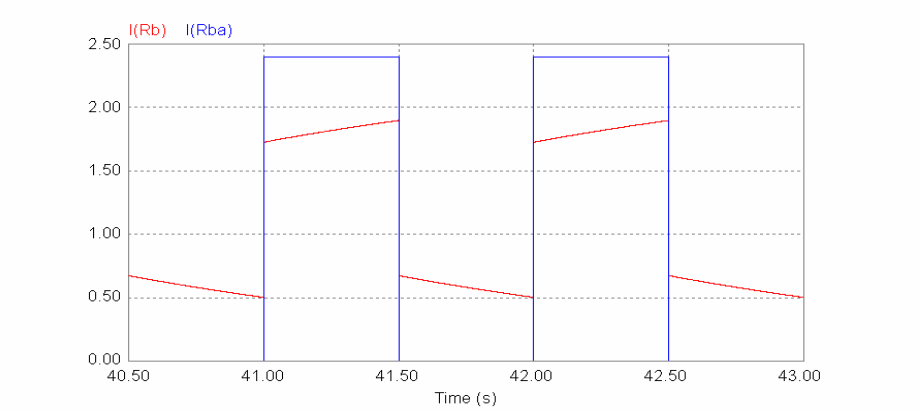

Figure 48 Battery current with and without a supercapacitor connected to its terminals

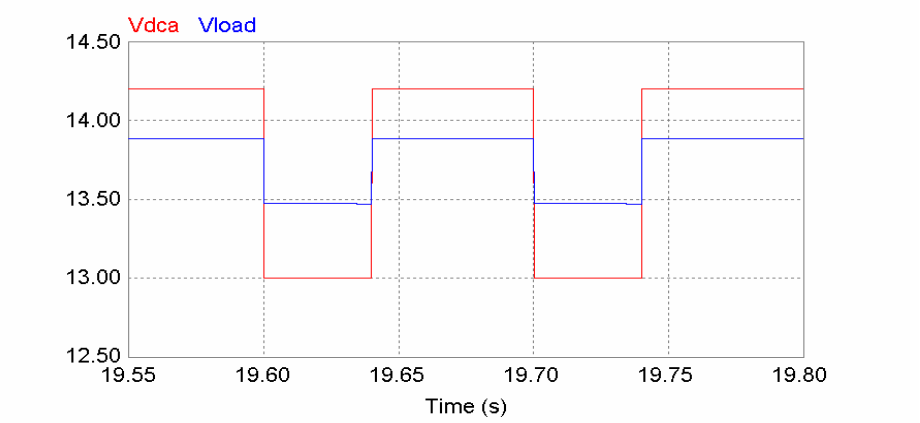

Figure 49 Voltage drop during conduction with and without a supercapacitor connected to the battery terminals

Now for the case of the second proposed approach to extend the battery run-time, the system was simulated using the same battery and supercapacitor bank than in the previous situation, but a 15mH inductor has been connected in series with the battery. In this case the resulting battery and supercapacitor currents are shown in figure 50. As can be observed from this result the rms current supplied by the battery is 1.33 A and its peak value is 1.8 A. Comparing these values with the battery current at stand alone

operation a reduction of a 12% in the rms current is achieved. Also the peak value of the current is reduces in a 26%.

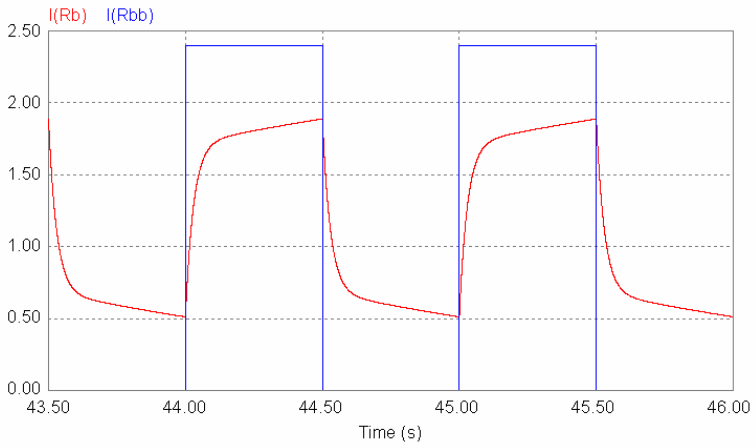

Figure 50 Battery current with and without a supercapacitor and inductor connected to its terminals

The third case simulated is using a dc-dc converter to interface the supercapacitor bank with the battery. For this simulation a 7.5V, 10 F, and 130 mΩ supercapacitor bank was used. The supercapacitor is connected to the battery terminals using a buck-boost converter working with a 50% duty cycle and a switching frequency of 20 kHz. The current being taken by the load is the same as in the previous cases. The simulation result is shown in figures 51. Figure 51 shows the current delivered by the battery with and without the supercapacitor connected. It can be observed that without the supercapacitor the current supplied by the battery is 1.51 A_{RMS} and it has a peak value of 2.4 A. In the case were the supercapacitor is connected the current delivered by the battery is 1.36 A_{RMS} and 2 A peak. Thus a reduction of a 9.9% in the current delivered

by the battery is achieved. This has an important effect in the extension of the battery run-time as can be seen in figure 47. In this case the battery discharge curve that has to be used corresponds to 0.9C instead of 1C.

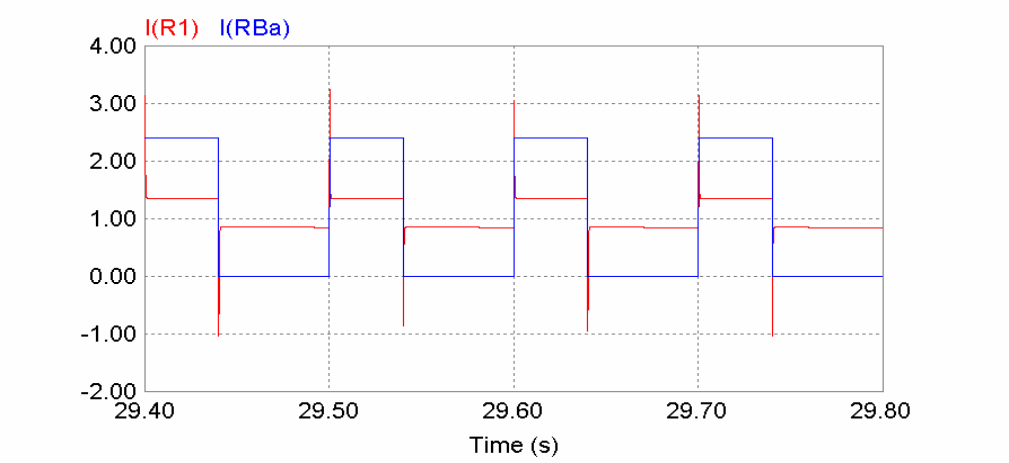

Figure 51 Battery current with and without a supercapacitor connected to its terminals when using a dc-dc converter

5.5. Experimental results

To validate the results obtained by means of simulation experimental measurements were taken in the laboratory. The first case under study is the normal battery performance. In this case the discharge characteristics of a laptop battery supplying energy to a typical mobile device current profile without and with a supercapacitor connected in parallel is studied. From the first test a run-time of 231 minutes was obtained. The second test conducted is the addition of 2 and 4 supercapacitor branches in parallel with the battery. To match the battery voltage every branch is composed by six 10 F 2.5 V supercapacitors connected in series. The

equivalent capacitance and ESR of the case when two supercapacitor branches are used is 3.34 F and its ESR is 390 mΩ. And the battery internal resistance is measured to be 500 mΩ. Figure 52 shows the current distribution between battery and super capacitor for this case. From this figure the peak current provided by the battery is reduced by 15%. The battery run-time for this condition was measured to be 240 minutes, which is a run-time extension of 4.3 %.

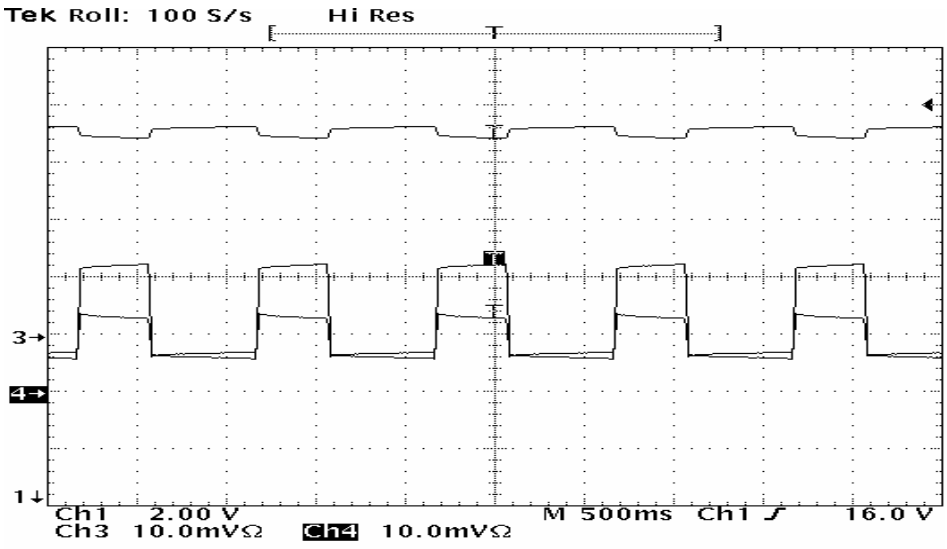

Figure 52 Battery and supercapacitor currents for two supercapacitor branches connected in parallel

The next situation tested is the addition of to more capacitor branches in parallel. The equivalent capacitance added is 6.68F with an ESR of 195 mΩ. The battery and capacitor current waveforms for this condition are shown in figure 53.

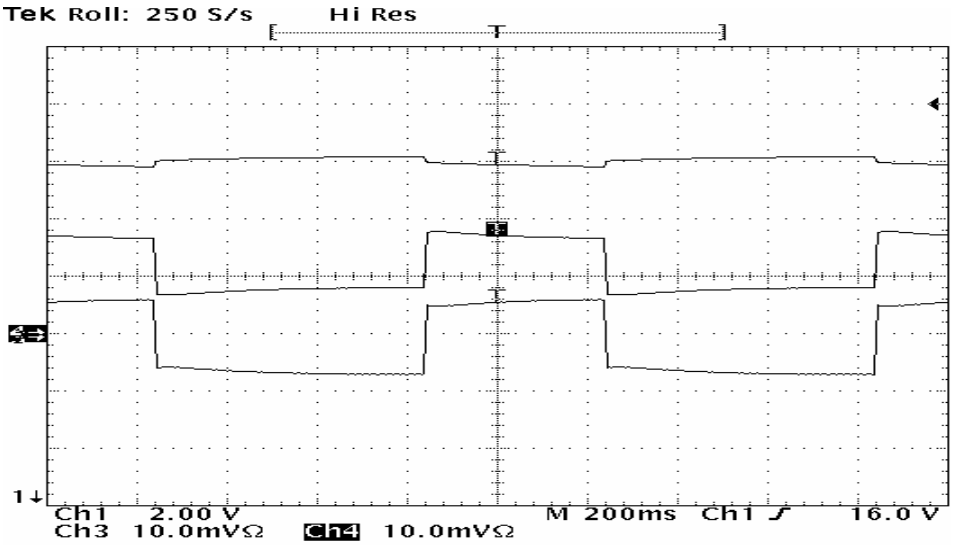

Figure 53 Battery and supercapacitor currents for four branches connected in parallel

From here it is possible to see that a reduction 11% in the battery rms current value is achieved. The run-time achieved for this configuration is 259 minutes; this is an improvement of a 12% over the normal battery run-time. The next case studied is the connection of an inductor in series with the battery to further increase the current redistribution between battery and capacitor. For this a 5mH inductor was used. Figure 54 shows the battery and capacitor currents for this case.

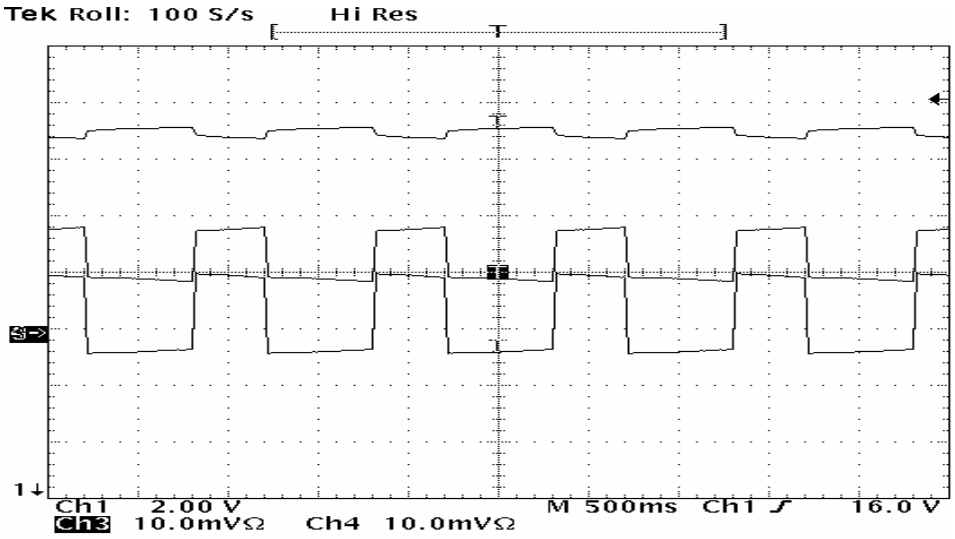

Figure 54 Battery and supercapacitor currents for four branches in parallel and inductor in series

The rms current provided by the battery was measured to be a 10% lower than the normal condition. The run-time in this case was 263 minutes, or a 13.8% longer than the normal case. The last condition under test is the use of a dc-dc converter to interface a low voltage supercapacitor bank with the battery. For this test a 7.5 V 10F, and 130 mΩ equivalent capacitor was used. The switching frequency of the dc-dc converter was set up to 20 kHz with a duty cycle of 50%. The current waveforms for the battery and capacitor are shown in Figure 55 below. The battery rms current is reduced by 8% as can be observed from this figure. The run-time in this case is 238 minutes or 3% more than the only the battery is used.

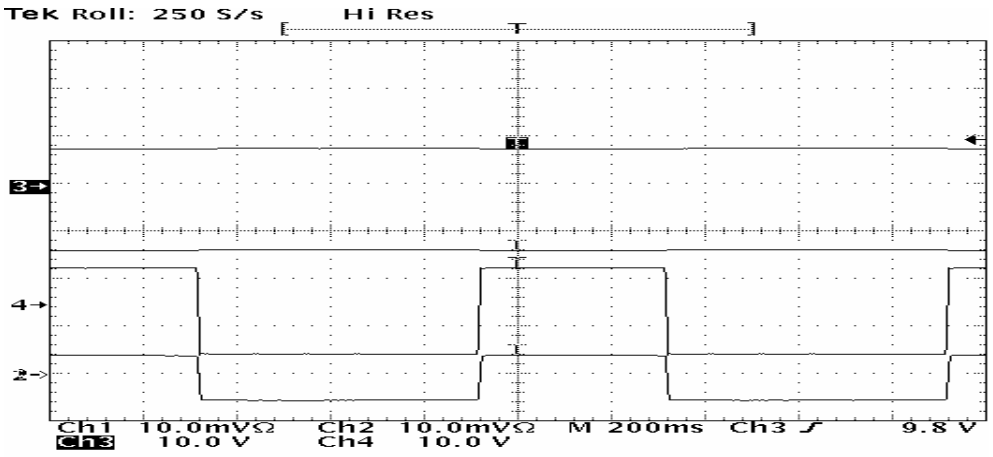

Figure 55 Battery and supercapacitor currents for one branch when using a dc-dc converter

Figure 56 shows the time versus voltage characteristics measured during the different test conditions. From here is it possible to conclude that adding an inductor can give an extra run-time extension of approximately 2% more time. Also it can be seen that the use of a dc-dc converter can achieve a similar performance in run-time extension than an equivalent supercapacitor having twice as many cells, as can be seen when comparing the voltage curve for two capacitor branches and the one for the dc-dc converter interface

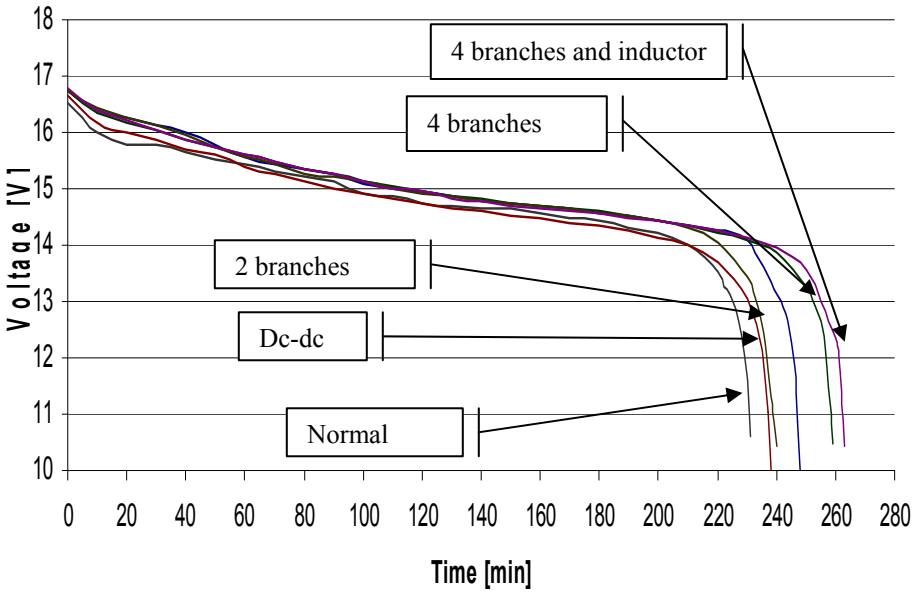

Figure 56 Battery voltage as function of time without and with a supercapacitor

5.6. Conclusions

In this Chapter the problem of the battery run-time extension has been addressed. The use of Supercapacitors to extend the run-time of a mobile device has been analyzed for three different approaches. The method of connecting directly the Supercapacitors to the battery terminals was analyzed and tested in a laboratory prototype. From the analysis it has been shown that the run-time extension obtained from the addition of capacitors in parallel depends on the number of capacitors being added. Also from this analysis it is possible to conclude that adding more than 5 supercapacitor branches in parallel has a marginal effect on the run-time extension. The analysis also shows that a reduction on the supercapacitor ESR can improve the run-time extension effect by further reducing internal loses and improving the battery current waveform.

From experimental tests performed in the laboratory extensions of 4% and 12% percent have been achieved The addition of an inductor in series with the battery increases the run-time of the system by an extra 2% when compared to a battery capacitor connection. This extra time is gained by the reduction in the peak value of the battery current. The use of a dc-dc converter to interface the supercapacitor bank and the battery results in a reduction of 50% of the capacitors needed to achieve the same run-time extension. This reduction is achieved mainly because of the smaller number of cells is needed to match the battery terminal voltage. Thus increasing the equivalent capacitance and reducing the equivalent ESR of the capacitor bank. Therefore increasing the power delivering capability of the system and reducing its internal loses.

CHAPTER VI

CONCLUSIONS

Several energy storage technologies are available today for use in power electronics, such as flywheels, high capacity batteries and supercapacitors. Among these three energy storage devices supercapacitors show some important advantages due to their high power density, low ESR, reduced size and weight. Supercapacitors, when compared to a more traditional energy storage device such as lead acid batteries have a power density 10 times higher. Also supercapacitors out perform batteries having an extended operational life with no degradation due deep discharge cycles.

The most important disadvantages being exhibit by supercapacitors are their low terminal voltage, which is 2.5 Volts per cell, and their low energy density. Having such a low cell voltage forces to stack them in connected in series to match the load voltage. This has the negative effect of increasing the equivalent ESR and reducing the capacitance of the resulting supercapacitor. Also the fact that supercapacitors have a low energy density makes this energy storage technology not suitable for long term energy backup.

Due to the low supercapacitor terminal voltage dc-dc converters are required to interface with higher voltage loads. Several dc-dc topologies are available to perform this function. For selecting the appropriate interfacing topology the most important

considerations are bidirectional power flow capability to maintain the supercapacitor state of charge, and the application specific load requirements. An other important point during the dc-dc converter topology selection process is the converter performance. For this evaluation the switch utilization index proves to be a useful tool.

The use of a supercapacitor bank to provide ride through in adjustable speed drives was tested in a laboratory prototype. The system performance proved to be good to compensate deep voltage sags as well as short voltage interruptions, while maintaining the dc link voltage level invariant during the duration of the transient disturbance. From the results shown in Chapter IV is clear that the supercapacitor dynamic response is fast enough to respond to the load transient requirements and avoid the effects of the voltage sags on the adjustable speed drive.

The use of a battery – supercapacitor hybrid connection proved to be beneficial for run-time extension in mobile applications. The run-time extension is achieved due to the reduction in the battery internal loses. This loss reduction is generated by the lower impedance resulting from the battery-supercapacitor connection. This loss reduction effect is accompanied by an improvement in the power delivering capability of the battery-supercapacitor system improving its performance for pulsating loads such as microprocessors. Three battery-supercapacitor connection methods were proposed and evaluated. It was shown that by the parallel connection of battery and supercapacitor a run-time extension of a 12% is achievable. Also it was found that he addition of an inductor connected in series with the battery in the previous case increases the run-time of the system by an extra 2% when compared to a parallel battery capacitor connection.

Further it was shown that the use of low voltage supercapacitor cells interfaced via a dc-dc converter allows the reduction of the number of supercapacitor cells required to extend the system run-time. Thus this has the effect of reducing the cost and size of the run-time extension approach.

Future improvements in the supercapacitor equivalent series resistance value will result in an extra run-time extension capability. This is due to a larger reduction in internal losses, and by improving the battery current shape. This is by reducing the peak and rms values of the battery current.

REFERENCES

[1] H.G. Sarmiento, E Estrada, "A voltage sag study in industry with adjustable speed drives", *IEEE Industry Applications Magazine*, vol. 2, no. 1, pp. 16-19 January /February 1996.

[2] N. Mohan, T. M. Underland and W.P. Robbins, *Power Electronics, Converters, Applications and Design*, New York: John Wiley & Sons, 1995.

[3] M. H. J. Bollen, "Voltage sags effects, mitigation and prediction", *Power Engineering Journal,* vol. 10, no. 3, pp. 129 -135, June 1996.

[4] D. Cahela, B. Tatarchuk, "Overview of electrochemical double layer capacitors", in *Conf. Rec. IEEE-IECON' 97,* 1997, pp. 1068 -1073

[5] F. Belhachemi, S Rael, B. Davat, "A physical based model of power electric double-layer supercapacitors", in *Conf. Rec IEEE-IAS'2000,* 2000, pp. 3069-3076.

[6] T.A. Smith, J.P. Mars, G.A. Turner, "Using supercapacitors to improve battery performance", in *Conf. Rec. IEEE-PESC'02*, 2002, pp. 124-128.

[7] F. Nome, I. Barbi, " A ZVS Clamping mode-current-fed push-pull dc-dc converter", in *Conf. Rec. IEEE-IAS'00*, 2000, pp. 3069-3076.

[8] A. Rabello, M. Co, D. Simonetti, J. Vieira, " An isolated dc-dc boost converter using two cascade control loops", in *Conf. Rec. IEEE-ISIE '97*, 1997, pp. 452 -456.

[9] W. de Argano, I. Barbi, "A comparison between two current-fed push-pull dc-dc converters – Analysis, design and experimentation", in *Conf. Rec. IEEE -INTELEC '96*, 1996, pp. 313 -320.

[10] A. Rabello, M. Co, G. Sousa, J. Vieira, "A fully protected push-pull current-fed dc-dc converter", in *Conf. Rec. IEEE-IECON 97*, 1997, pp. 587 -592.

[11] D. Divan, W. Brumsickle, "Powering the next millennium with power electronics", in *Conf. Rec. IEEE-PEDS '99*, 1999, pp. 7 -10.

[12] N.S. Tunaboylu, E. R. Collins Jr. and S. W. Midlekauff, "Ride-through issues for the motor drives during voltage sags", in *Conf. Rec. IEEE Southeastcon '95*, 1995, pp. 26-29.

[13] Maxwell Technologies, (Accessed May 2002) "Power Cache ultracapacitors data sheet" [Online]. Available: http://www.maxwell.com

[14] Montena Components, (Accessed June 2002) “BOOSTCAP series data sheet” [Online]. Available: http://www.montena.com.

[15] Koldban Capacitors, (Accessed June 2002) “KBi power data sheet” [Online]. Available: http://www.koldban.com.

[16] P.H. Mellor, N. Schofield, D. Howe, “ Flywheel and supercapacitor peak power buffer technologies”, in *Conf. Rec. IEEE Electric, Hybrid and Fuel Cell Vehicles*, 2000, pp. 8/1 -8/5.

[17] Paulo Ribeiro, Brian Johonson, Mariesa Crow, Aysen Arsoy, Yilu Liu, “ Energy storage systems for advanced power applications”, *Proceedings of the IEEE* , vol. 89 no. 12 , pp. 1744 -1756, Dec. 2001.

[18] D. Panigraphi, C. Chiasserini, S. Dey, R. Rao, A. Raghunthan and K. Lahiri, “Battery life estimation of mobile embedded systems”, in *Conf. Rec. 14th Annual Conference in VLSI Design*, 2001, pp. 57 -63.

[19] L. Benini, G. Castelli, A. Macci, E. Macci, M. Poncino, R. Scarsi, “ A discrete-time model for high-level power estimation”, in *Conf. Rec. 7th Asia and South Pacific and the 15th International Conference on VLSI Design ASP-DAC’02*, 2002, pp. 261 - 267.

[20] H.L. Chan, D. Sutanto, “A new battery model for use with battery energy storage systems and electric vehicles power systems”, in *Conf. Rec. IEEE Power Engineering Society Winter Meeting*, 2000, pp. 470 -475.

[21] EPCOS Components, (Accessed February 2003) “Ultra cap series data sheet” [Online]. Available: http://www.epcos.com.

APPENDIX A

SMALL CELL SUPERCAPACITOR DATASHEETS

Features:

- Delivers up to 100 times the energy of conventional capacitors and delivers ten times the power of ordinary batteries
- Is optimized for individual applications through its capacity to repeatedly charge and discharge
- Designed for smaller and lighter-weight products
- Offers instantaneous ride-through power
- UL recognized

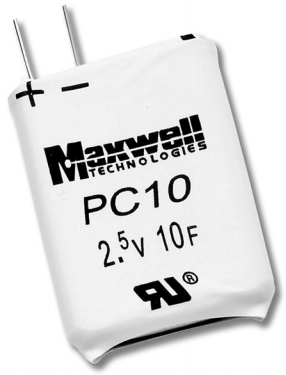

PC10

BOOSTCAP® Ultracapacitor

BOOSTCAP® Ultracapacitors provide extended power availability, allowing critical information and functions to remain available during dips, sags, and outages in the main power source. In addition, it can relieve batteries of burst power functions, thereby reducing costs and maximizing space and energy efficiency. The ultracapacitor features a cylindrical design and an electrostatic storage capability that can cycle hundreds of thousands of charges and discharges without performance degradation.

BATTERY vs. ULTRACAPACITOR vs. CAPACITOR COMPARISON

Available Performance	*Lead Acid Battery*	*Ultracapacitor*	*Conventional Capacitor*
Charge Time	1 to 5 hours	0.3 to 30 seconds	10-3 to 10-6 seconds
Discharge Time	0.3 to 3 hours	0.3 to 30 seconds	10-3 to 10-6 seconds
Energy (Wh/kg)	10 to 100	1 to 10	‹0.1
Cycle Life	1,000	›500,000	›500,000
Specific Power (W/kg)	‹1000	‹10,000	‹100,000
Charge/discharge efficiency	0.7 to 0.85	0.85 to 0.98	›0.95

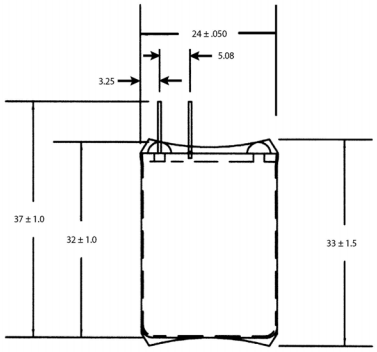

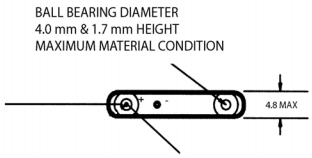

NOTES:
1) DIMENSIONS ARE IN (mm)
2) TOLERANCES ARE +/- .5 UNLESS OTHERWISE SPECIFIED
3) PIN DIA .500 +/- .05 mm

Specifications

Capacitance	• 10 Farads	(DCC, 25°C)	
Capacitance Tolerance	• -10%/+30%		
Voltage			
Continuous	• 2.5 V		
Peak	• 2.7 V		
Series Resistance			
DC	• 180 mΩ	(-25%/+25%)	
1 kHz	• 61 mΩ	(-25%/+25%)	
Current (Rated) [1,2]	• 2.5 A		
Stored Energy	• 31 J		
Leakage Current	• 0.040 mA	(72h, 25°C)	
Weight	• 6.4 g		
Volume	• .003 L		
Temperature [3]			
Operating	• -40° C to 70° C		
Storage	• -40° C to 85° C		
Life Time (25°C)	• 10 y	ΔC >20%, ESR < 200% of initial value	
Cyclability (25°C, I = 20 A)	• 500,000	ΔC >20%, ESR < 200% of initial value	

With a capacitance of 10 farads at 2.5 volts, and in a 24 x 33 x 4.5 mm package, the UL recognized PC10 ultracapacitor is ideal for consumer electronics, automotive subsystems, wireless transmission, medical devices, automatic meter readers, and many other applications requiring a pulse of energy that cannot be efficiently provided by a battery or power supply alone. The PC10 works in tandem with batteries for applications that require both a constant low power discharge for continual function and a pulse power for peak loads. In these applications, the device relieves batteries of peak power functions resulting in an extension of battery life and a reduction of overall battery size and cost.

The PC10 is also an ideal source of back-up power and pulse. It can provide extended power availability, allowing critical information and functions to remain available during dips, sags, and outages in a power supply or battery change. The PC10 is capable of accepting changes at the identical rate of discharge.

Physical Characteristics

Dimensions (Reference only)	• 24 x 33 x 4.5 mm	(+/- 1 mm)

NOTES

[1] Rated current: 5 sec discharge rate to ½V
[2] Device can withstand short circuit current if kept within the operating temperature
[3] Steady state case temperature

Worldwide Headquarters

MAXWELL TECHNOLOGIES
9244 Balboa Avenue • San Diego, 92123 CA, USA
PHONE: +(1) 858 503 3300
FAX: +(1) 858 503 3301
EMAIL: ultracapacitors@maxwell.com

European Office

MAXWELL TECHNOLOGIES SA
CH-1728 Rossens • Switzerland
PHONE: +41 (0) 26 411 85 00
FAX: +41 (0) 26 411 85 05
EMAIL: ultracapacitors@maxwell.com

www.maxwell.com

EPCOS

UltraCap 10F/2.3V

Preliminary technical data			
Rated Capacitance (DCC[1], 25°C)	C_R	10	F
Capacitance Tolerance		–10…+30	%
Rated Voltage	U_R	2.3	V
Specific Power (matched load)		1.9 kW/kg; 3.9 kW/l	
Rated Current (25°C)	I_C	3	A
Stored Energy (at U_R)	E	26.5	J
Specific Energy (at U_R)		1.2 Wh/kg; 2.4 Wh/l	
Surge Voltage	U_S	2.7	V
Max. Leakage Current (72h, 25°C)	I_{LC}	40	µA
Max. Series Resistance (25°C)	ESR	110	mΩ
Max. Series Resistance (25°C)	ESR_{DC}	180	mΩ
Weight		6.4	g
Volume		0.0031	l
Operating Temperature	T_{op}	–30…+70	°C
Storage Temperature	T_{st}	–40…+70	°C
Lifetime (25°C, U_R)	$t_{LD(Co)}$	90 000 h	Criteria: |ΔC| > 20% of initial value or ESR > 200% of initial value or ILC > specified value
Lifetime, cycles[2] (25°C, I_C = 1 A)	$t_{LD(Cl)}$	500 000	

Remarks: 1) DCC: discharging with constant current
2) 1 cycle: charging to U_R, 30 s rest, discharging to 0 V, 30 s rest

Product

Features

- Prismatic cell
- Solderable pins

Type	B49100
Ordering code	B49100A1104Q000
Voltage	2.3 V
Capacitance	10 F
Dimensions (mm)	D: 4.7 ± 0.2
	W: 23.5 ± 0.5
	L: 29.0 ± 1.0

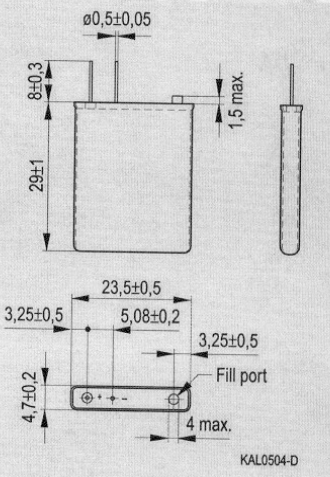

Cells

EPCOS

UltraCap 10F/2.3V

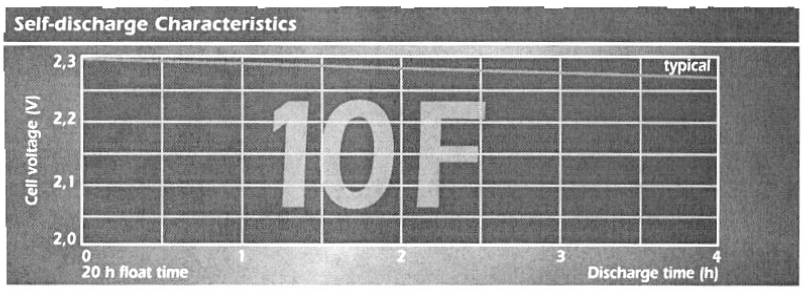

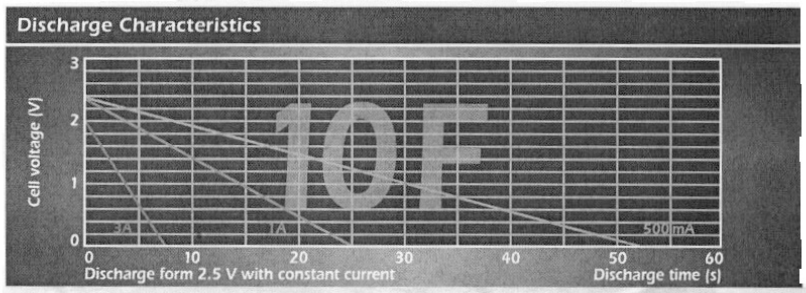

APPENDIX B

BIG CELL SUPERCAPACITOR DATASHEETS

Features:

- Long lifetime of several hundred thousand cycles
- Fast charging with high currents and very high discharge currents
- Resistant against reverse polarity
- Ultra-low internal resistance
- Environmentally friendly
- Low weight and volume
- Shock- and vibration-proof

BCAP0010

BOOSTCAP® Ultracapacitor

BOOSTCAP® Ultracapacitors provide extended power availability, allowing critical information and functions to remain available during dips, sags, and outages in the main power source. In addition, it can relieve batteries of burst power functions, thereby reducing costs and maximizing space and energy efficiency. The ultracapacitor features a cylindrical design and an electrostatic storage capability that can cycle hundreds of thousands of charges and discharges without performance degradation.

BATTERY vs. ULTRACAPACITOR vs. CAPACITOR COMPARISON

Available Performance	*Lead Acid Battery*	*Ultracapacitor*	*Conventional Capacitor*
Charge Time	1 to 5 hours	0.3 to 30 seconds	10-3 to 10-6 seconds
Discharge Time	0.3 to 3 hours	0.3 to 30 seconds	10-3 to 10-6 seconds
Energy (Wh/kg)	10 to 100	1 to 10	‹0.1
Cycle Life	1,000	›500,000	›500,000
Specific Power (W/kg)	‹1000	‹10,000	‹100,000
Charge/discharge efficiency	0.7 to 0.85	0.85 to 0.98	›0.95

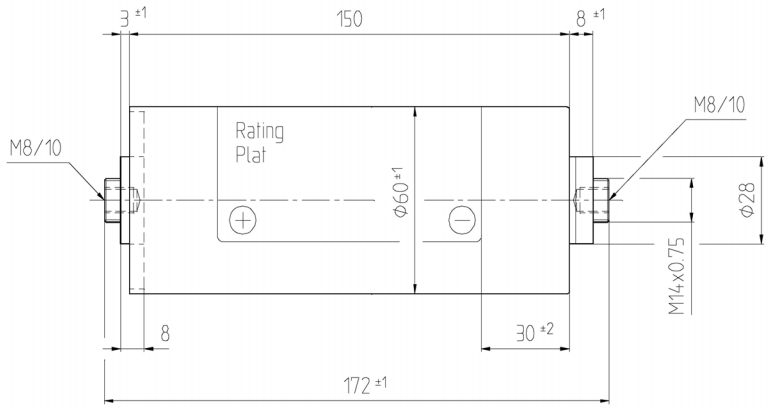

Specifications

Capacitance	• 2,600 Farads	(DCC, 25°C)
Capacitance Tolerance	• +20%/-20%	
Voltage		
Rated	• 2.5 V	
Surge	• 2.8 V	
Series Resistance (Maximum)	• 0.7 mΩ	(DCC, 25°C)
Specific Power Density	• 4,300 (W/kg)	(2.5 V)
Current (Maximum)	• 600 A	
Stored Energy (Maximum)	• 8,125 J	
Specific Energy Density	• 4.3 (Wh/kg)	(2.5 V)
Leakage Current (Maximum)	• 5 mA	(12h, 25°C)
Weight	• 525 g	
Volume	• 0.42 L	
Temperature[1]		
Operating	• -35° C to 65° C	
Storage	• -35° C to 65° C	
Life Time (25°C)	• 10 y	ΔC >20%, ESR < 200% of initial value
Cyclability (25°C, I = 20 A)	• 500,000	ΔC >20%, ESR < 200% of initial value

With a capacitance of 2600 farads at 2.5 volts, and in a cylindrical 60 x 172 mm package, Maxwell's BCAP0010 ultracapacitor is ideal for automotive subsystems, medical devices, UPS/backup power, and many other applications requiring a pulse of energy that cannot be efficiently provided by a battery or power supply alone.

The BCAP0010 works in tandem with batteries for applications that require both a constant low power discharge for continual function and a pulse power for peak loads. In these applications, the device relieves batteries of peak power functions resulting in an extension of battery life and a reduction of overall battery size and cost.

The BCAP0010 is also an ideal source of back-up power and pulse. It can provide extended power availability, allowing critical information and functions to remain available during dips, sags, and outages in a power supply or battery change. And, like all Maxwell ultracapacitors, the BCAP0010 is capable of accepting changes at the identical rate of discharge.

Physical Characteristics

Dimensions (Reference only)	• 60 x 172 mm (+/- 1 mm)
Screw Terminals	• M8/10mm
Electrical Connections	• M8/10mm Internal Threads
Torque (Maximum)	• 10Nm
General Tolerance	• ISO2768-v

Worldwide Headquarters

MAXWELL TECHNOLOGIES
9244 Balboa Avenue • San Diego, 92123 CA, USA
PHONE: +(1) 858 503 3300
FAX: +(1) 858 503 3301
EMAIL: ultracapacitors@maxwell.com

European Office

MAXWELL TECHNOLOGIES SA
CH-1728 Rossens • Switzerland
PHONE: +41 (0) 26 411 85 00
FAX: +41 (0) 26 411 85 05
EMAIL: ultracapacitors@maxwell.com

www.maxwell.com

EPCOS

UltraCap 2700F/2.5V

Preliminary technical data			New
Rated Capacitance (DCC[1]), 25°C)	C_R	2700	F
Capacitance Tolerance		–10...+30	%
Rated Voltage	U_R	2.5	V
Specific Power (matched load)		11.3 kW/kg; 13.0 kW/l	
Rated Current (25°C)	I_C	500	A
Stored Energy (at U_R)	E	8438	J
Specific Energy (at U_R)		3.9 Wh/kg; 4.5 Wh/l	
Surge Voltage	U_S	2.8	V
Max. Leakage Current (12h, 25°C)	I_{LC}		mA
Max. Series Resistance (25°C)	ESR	230	µΩ
Max. Series Resistance (25°C)	ESR_{DC}	300	µΩ
Weight		600	g
Volume		0.52	l
Operating Temperature	T_{op}	–35...+70	°C
Storage Temperature	T_{st}	–40...+70	°C
Lifetime (25°C, U_R)	$t_{LD(Co)}$		Criteria: |ΔC| > 30% of initial value or ESR > 200% of initial value or ILC > specified value
Lifetime, cycles (25°C, I_C = 100 A)	$t_{LD(Cl)}$		

Remarks: 1) DCC: discharging with constant current

Features

- Screw terminals
- AN-electrolyte

Type	B49400
Ordering code	B49400A2276Q002
Voltage	2.5 V
Capacitance	2700 F
Dimensions (mm)	D: 90.0 ± 1.0
	L: 82.0 ± 2.0

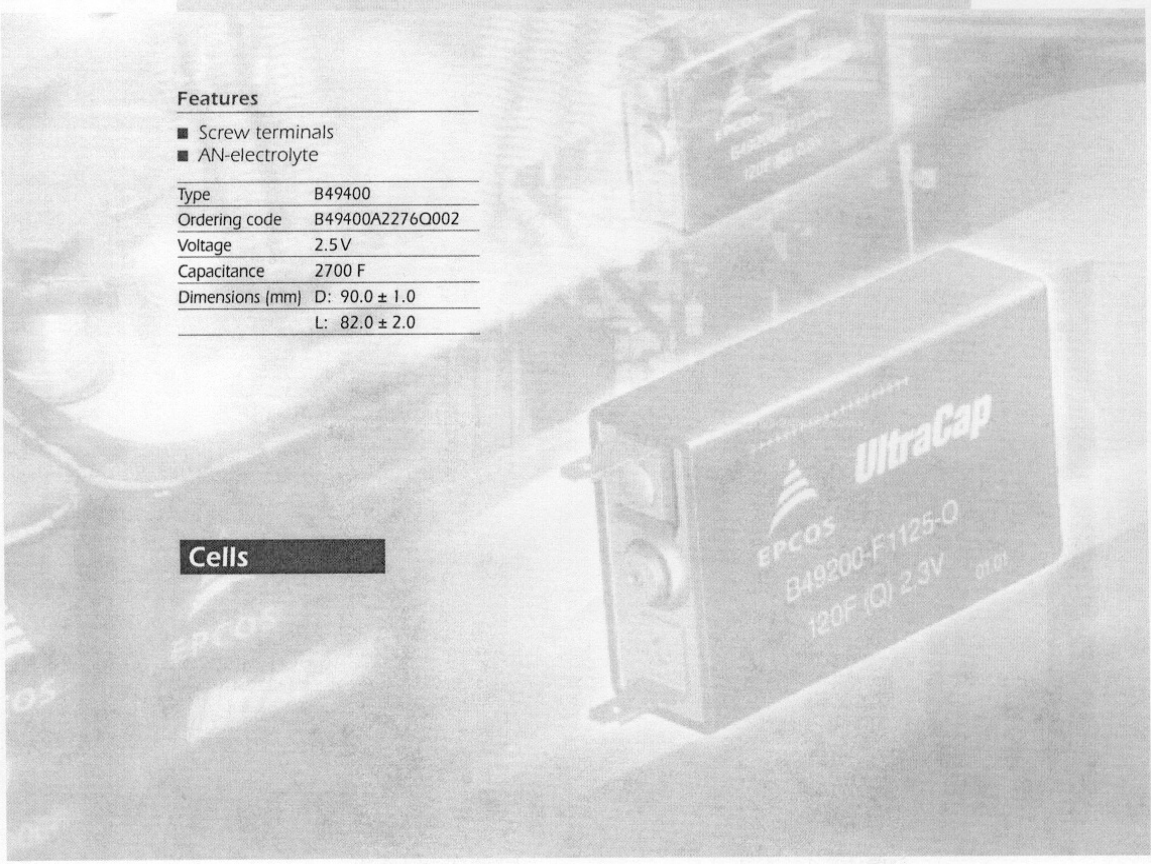

Cells

EPCOS

UltraCap 2700F/2.5V

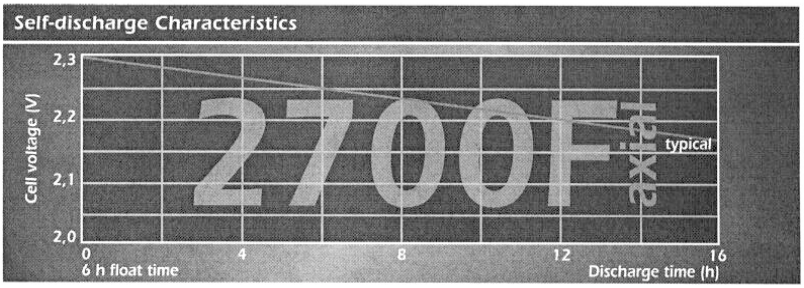

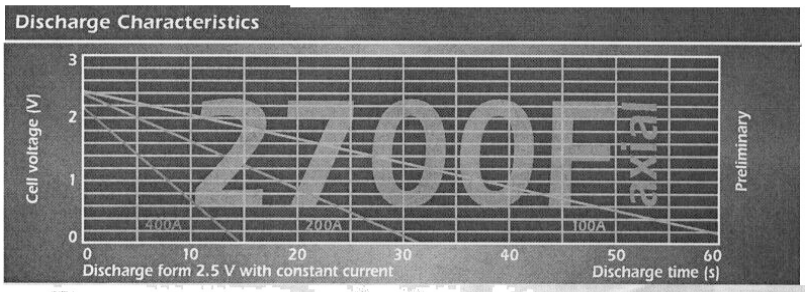

VITA

Leonardo Manuel Palma Fanjul graduated with a Bachelor of Engineering from Universidad de Concepción, Concepción, Chile in 1999. During the year 2000 he worked as a part-time engineer doing consulting. He joined the master's program in Electrical Engineering at Texas A&M University in January 2001, and received his Master of Science degree in August 2003.

His interests include power electronics, motor drives, energy storage devices, control systems and alternative energy applications.

He can be reached at palma@ieee.org or through the Department of Electrical Engineering, Texas A&M University, College Station, TX 77843, mail stop 77843-3128.